

**Dark matter annihilation and  
non-thermal processes  
in Galaxy clusters**

**Lidia Pieri**

**GGI workshop on Dark Matter  
May 7<sup>th</sup> 2010**



# The Coma galaxy cluster

$$D = 100 \text{ Mpc}$$

$$M_{\text{DM}} = 1.2 \times 10^{15} M_{\text{sun}}$$

$$R_{\text{vir}} = 2.7 \text{ Mpc}$$

$$B(r) = 4.7 n_{\text{th}}(r)^{0.5} \mu\text{G}$$

$$\langle B \rangle = 2 \mu\text{G}$$

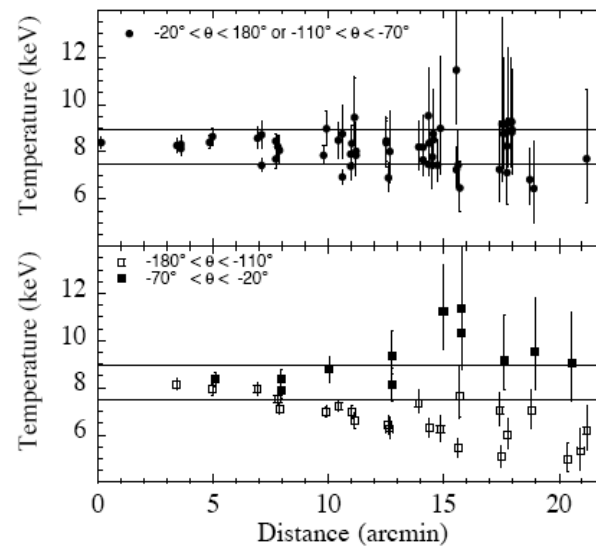
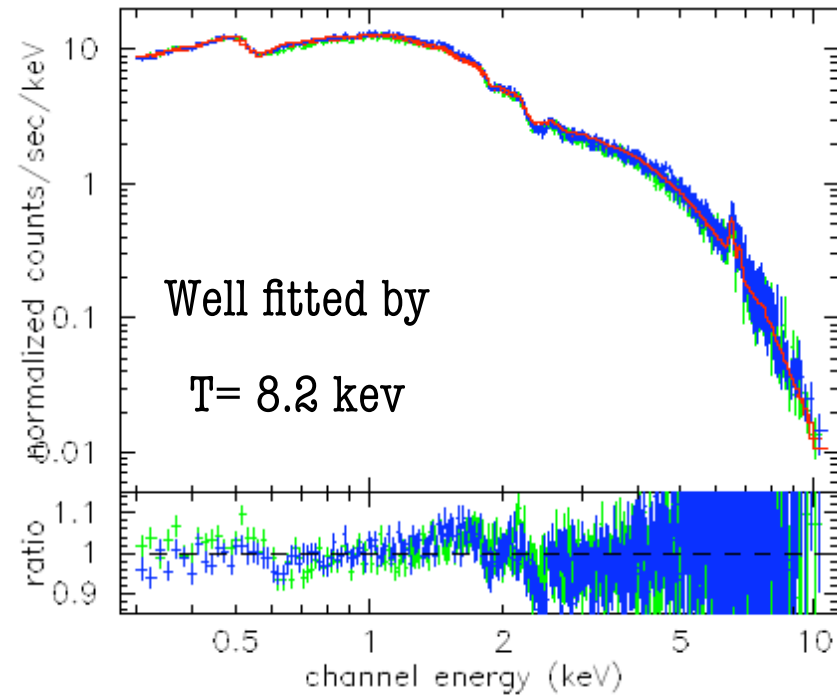
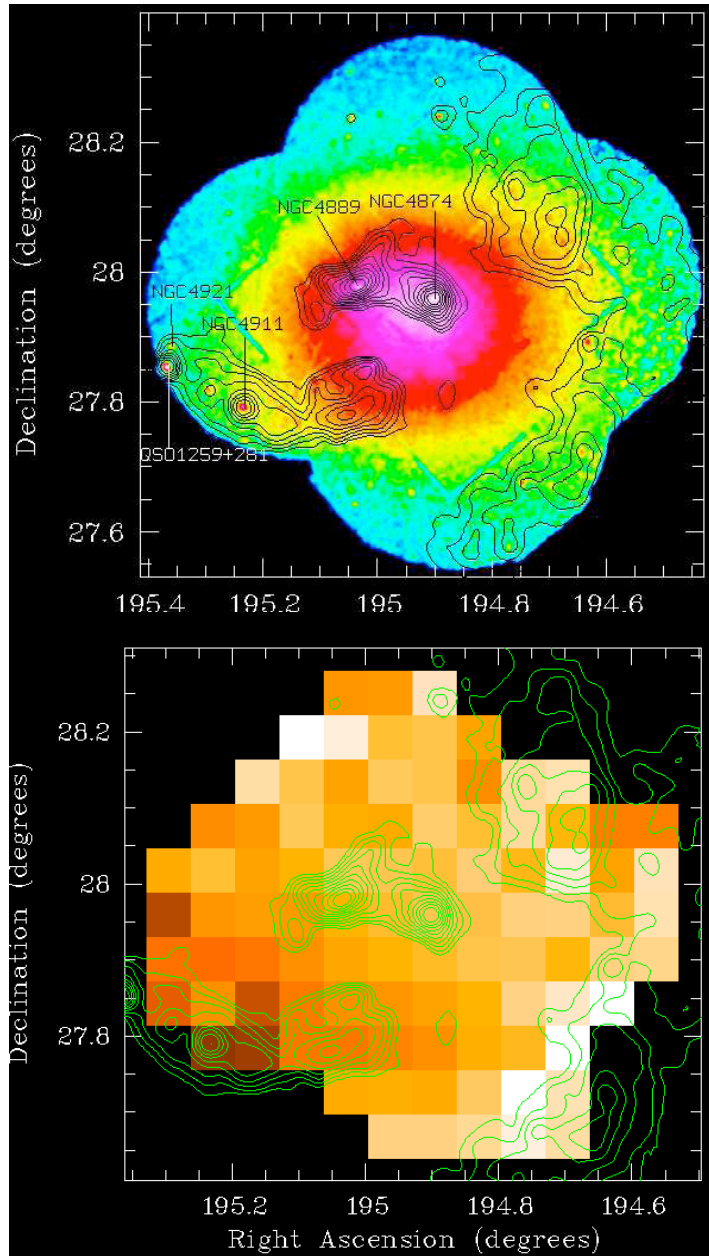
No cooling flow observed

Radio, EUV, X-ray observation



# The thermal component (from X-rays)

XMM [0.3 -2] keV

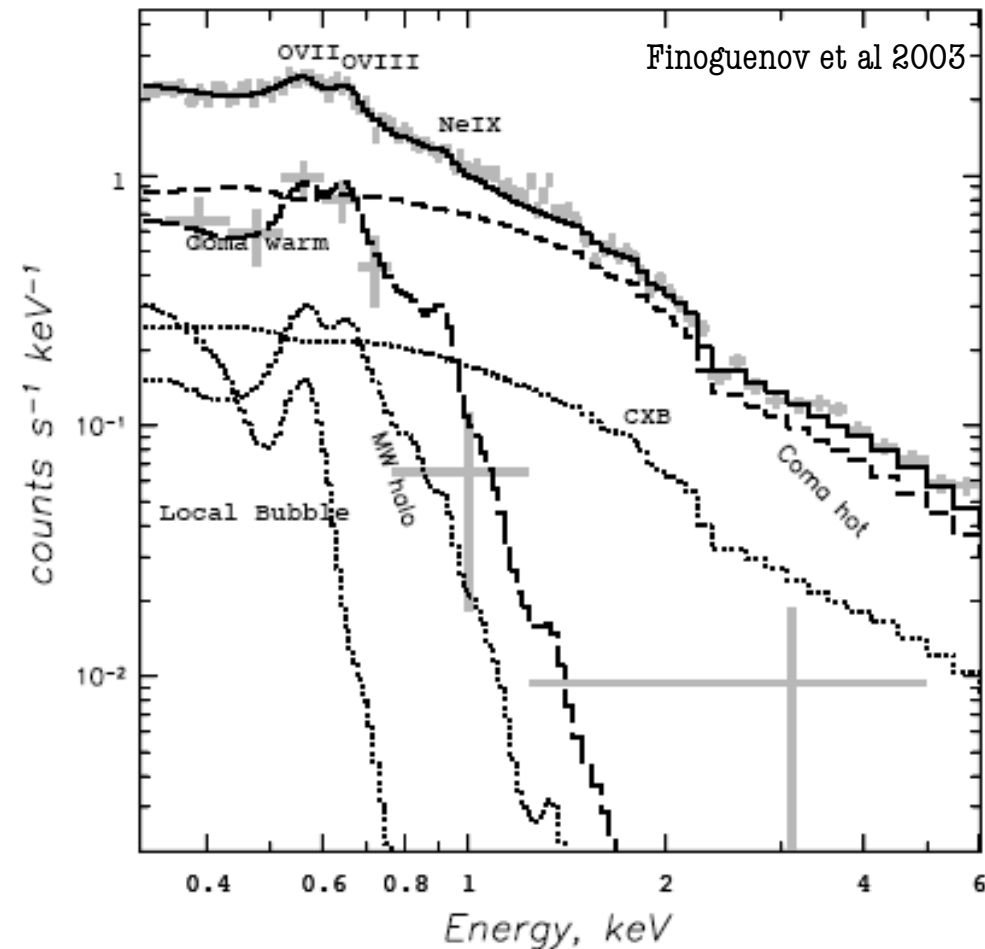




# Maybe a second thermal component

## The soft-X-ray excess in the outskirts of Coma ( $r > 1$ Mpc)

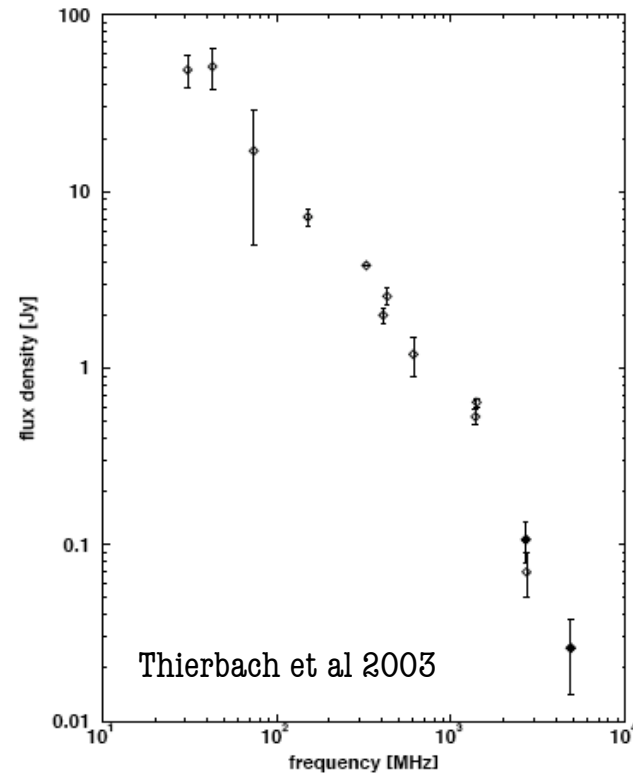
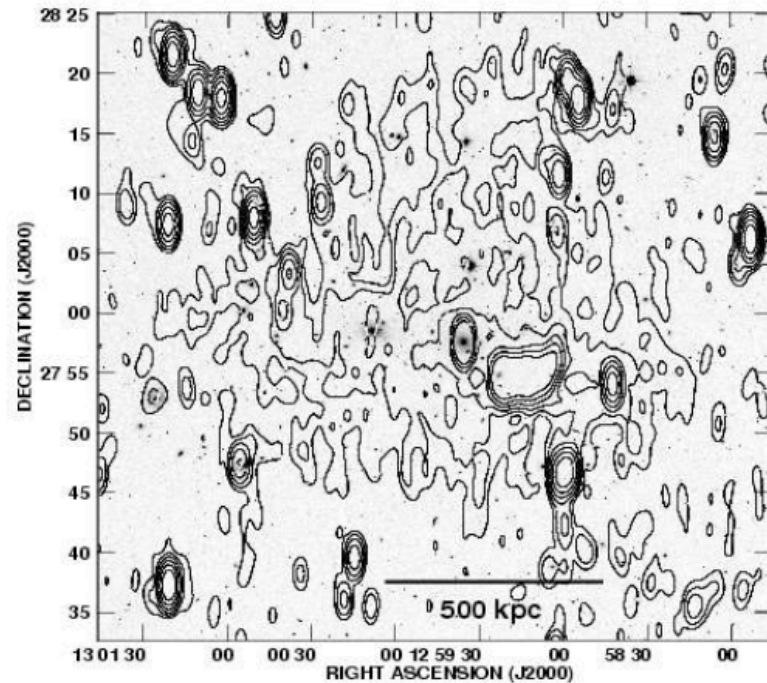
Fitted by a second thermal component of  $T = 0.22$  keV  
consistent with Warm-Hot Intergalactic Medium filaments found in numerical simulation of cluster formation





# Non-thermal components: the radio halo of Coma ( $r < 1$ Mpc)

Giovanini et al 1993



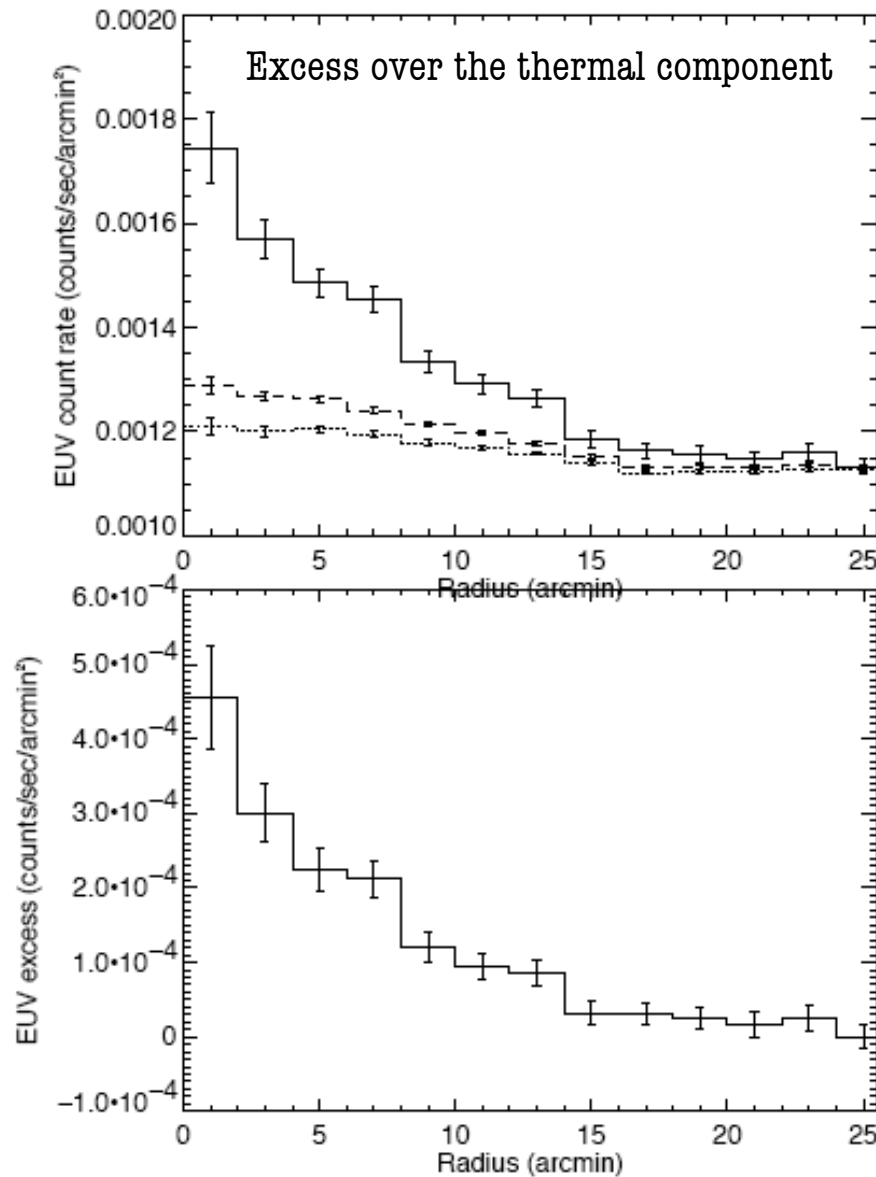
**Diffused over Mpc scale - Requires a population of relativistic non-thermal electrons  $\gamma > 10^4$  for  $B \sim 0.1, 1 \mu\text{G}$**   
(Note, Faraday Rotation Measurements suggest  $\langle B \rangle \sim 2 \mu\text{G}$  - Bonafede et al. 2010)

**Primary or reacceleration model:** electrons produced by AGN activity (quasars, radio galaxies) or star formation (supernovae, galactic wind, etc). Synchrotron and ICS radiation losses should be balanced by reacceleration (shock waves or magneto-hydrodynamics turbulences) - see Brunetti et al 2004 -

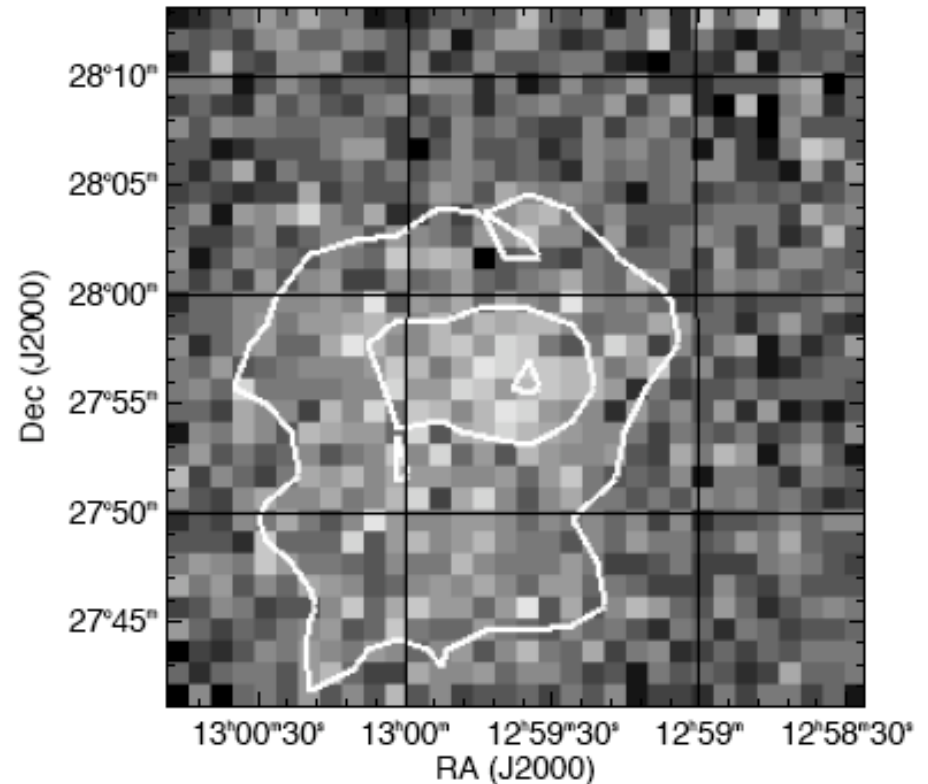
**Secondary model:** electrons produced in inelastic nuclear collisions between relativistic CR protons and thermal ions of the intracluster medium.  $B > \text{few } \mu\text{G}$  is needed + associated photon and neutrino production  
- see Blasi & Colafrancesco 1999 -



# The extreme UV excess in the center of Coma ( $r < 1$ Mpc)



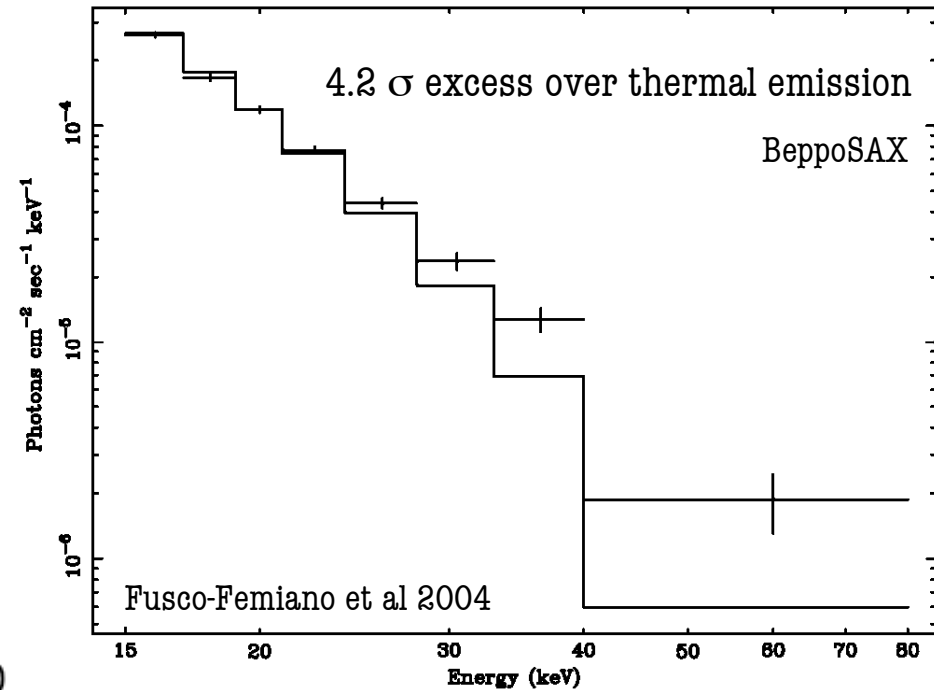
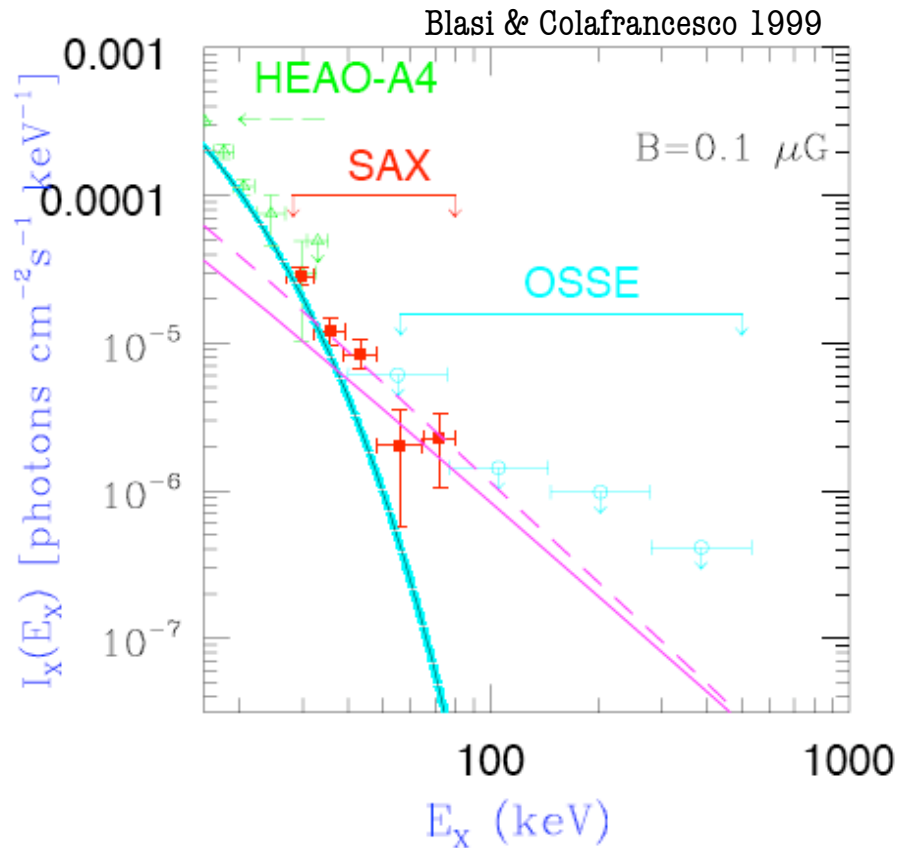
Possibly generated by a secondary population of relativistic electrons - produced through inelastic collisions of CRs with cluster plasma (secondary model) - which inverse Compton scatter off CMB photons



[0.13 - 0.18] keV

Bowyer et al 2004

## The hard X-ray excess in the center of Coma ( $r < 1$ Mpc)



Possibly generated by ICS off CMB of the same electrons responsible for the radio halo (primary or secondary).  
Warning: in case of secondary model, the magnetic field needed may overproduce  $\gamma$ -rays (Blasi&Colafrancesco 1999)

Alternative: maybe due to a supra-thermal electron tail developed in the thermal electron distribution due to stochastic acceleration in the turbulent intra-cluster medium (Ensslin et al 1998)



**Thermal gas at  $T=8.2$  keV**

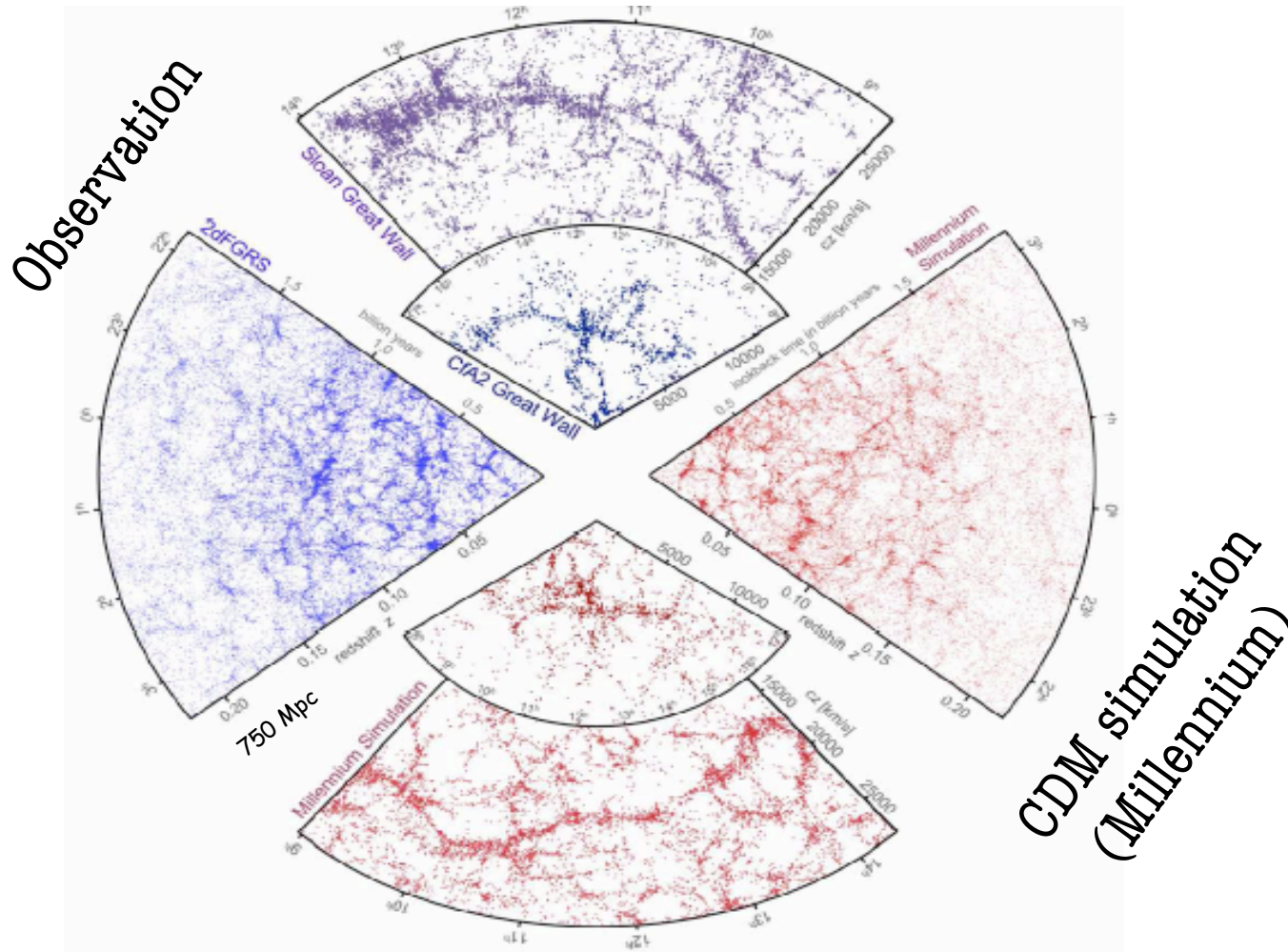
**Thermal gas in the filaments at  $T=0.22$  keV**

**Non-thermal electrons**

- 1) Produced by astrophysical source and continuously reaccelerated by cluster turbulences or merger shock waves
- 2) Produced by interaction of CRs with thermal ions



**An Alternative Non Thermal Hypothesis:  
(although non asked for...)  
Relativistic electrons are produced by DM annihilation**



# MILLENNIUM Simulation

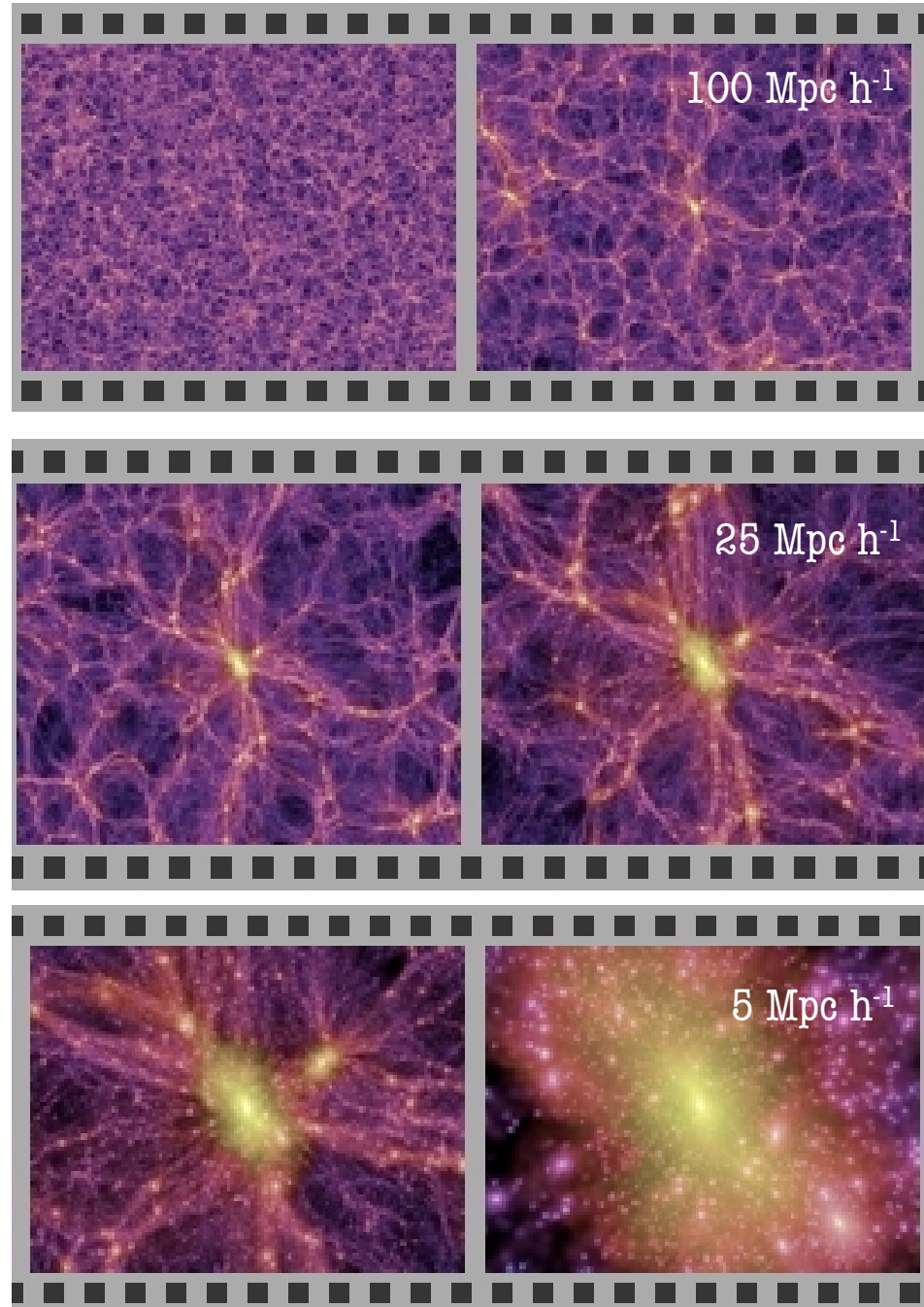
CDM universe

Springel et al. 2005

Simulates halos on cosmological scales, then resimulates a smaller patch with higher mass resolution down to cluster scale.

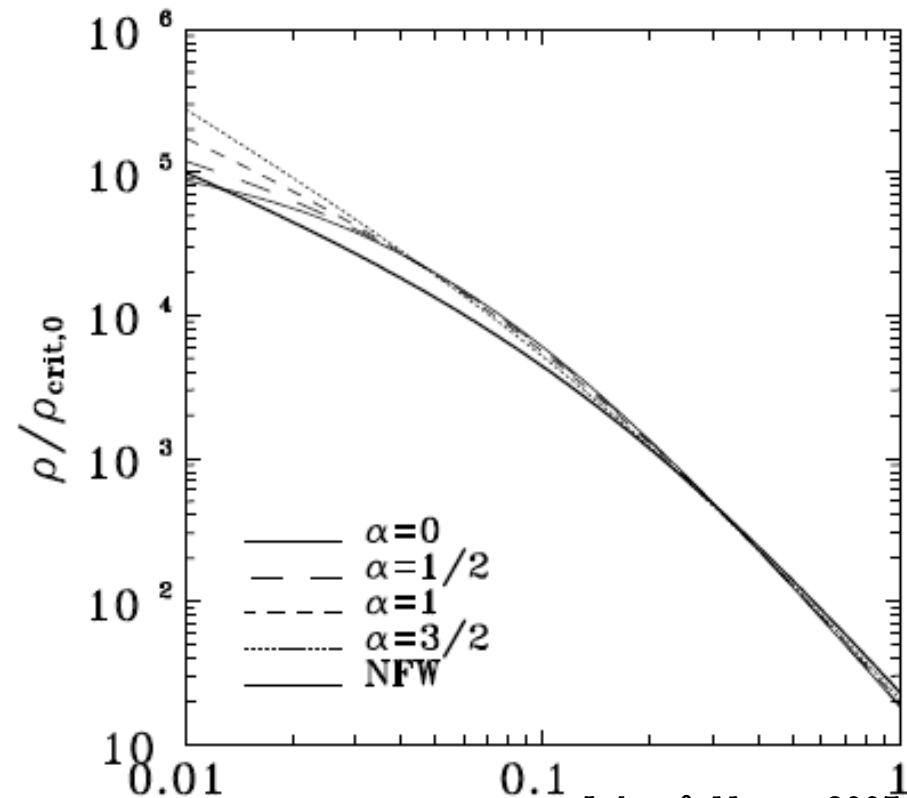
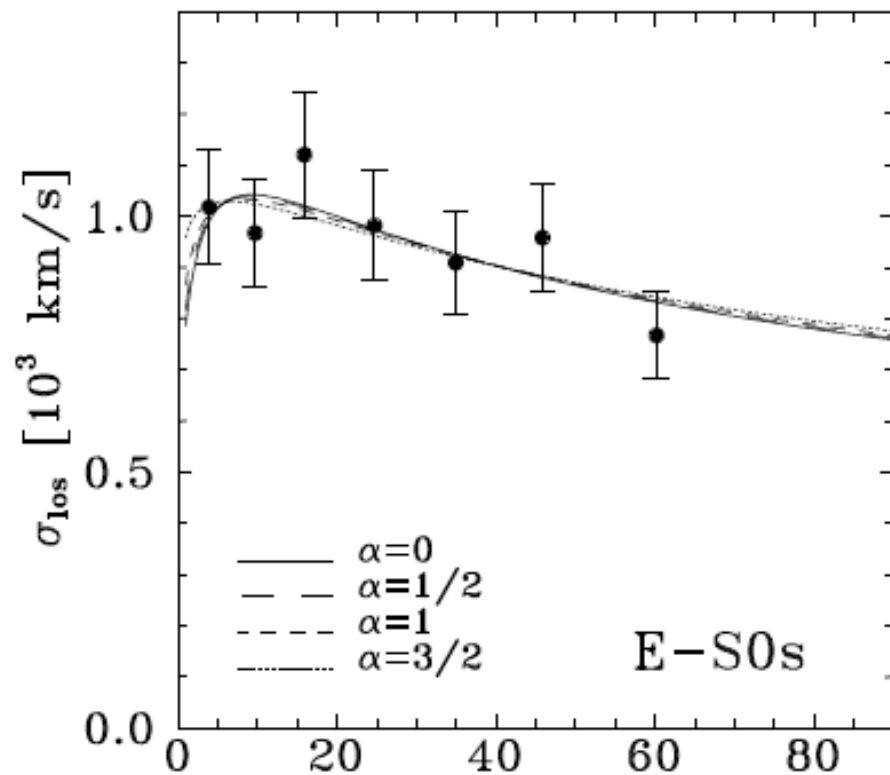
Tracks the formation of galaxies and quasars in the simulation, by implementing a semianalytic model to follow gas, star and supermassive black hole processes within the merger history trees of dark matter halos and their substructures

$z=0$



**An Alternative Non Thermal Hypothesis:  
(although non asked for...)  
Relativistic electrons are produced by DM annihilation**

DM Density profiles can be inferred from astronomical measurements  
or derived from numerical simulations

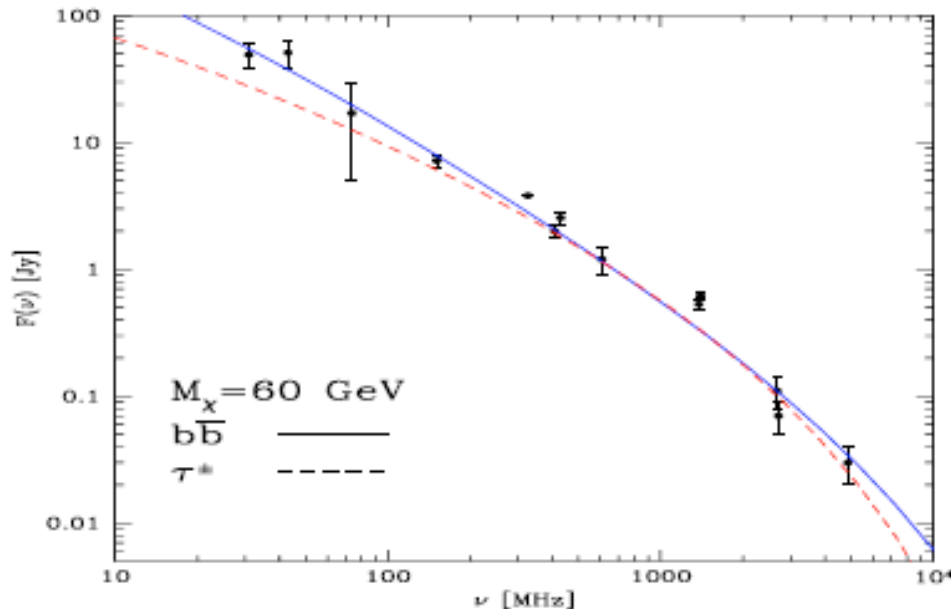
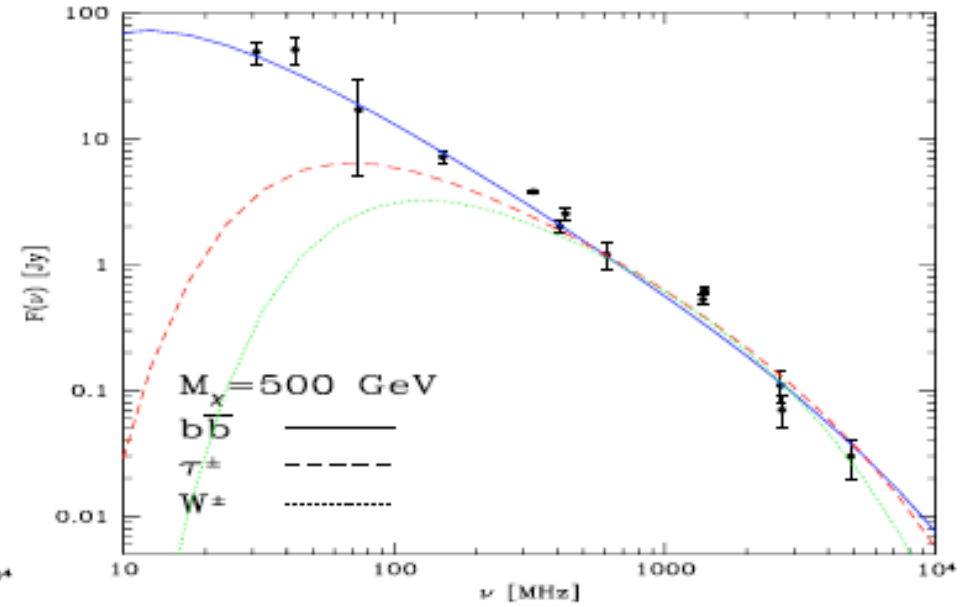
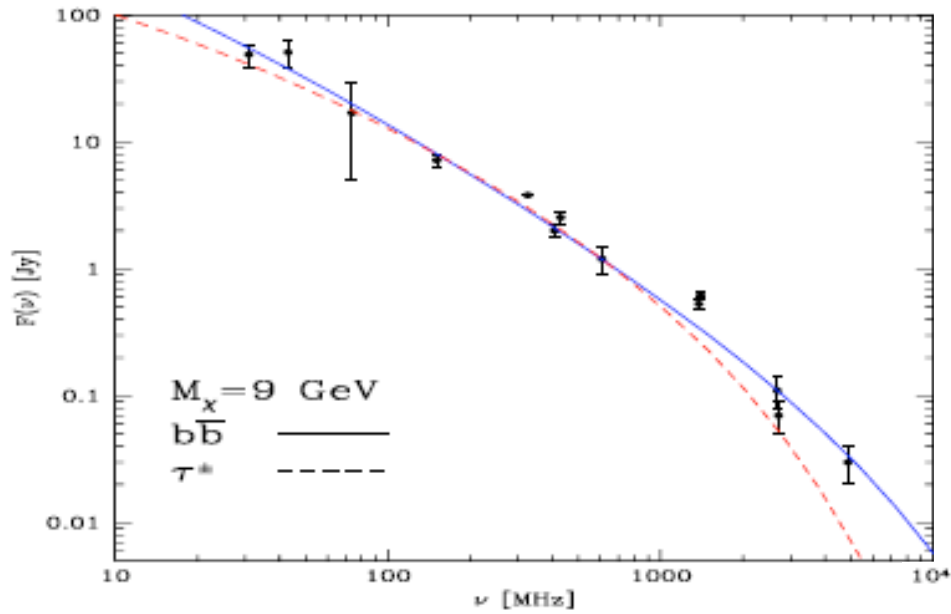


Lokas & Mamon 2003

Bullock et al 2001



# DM best fit to the radio halo spectrum of Coma



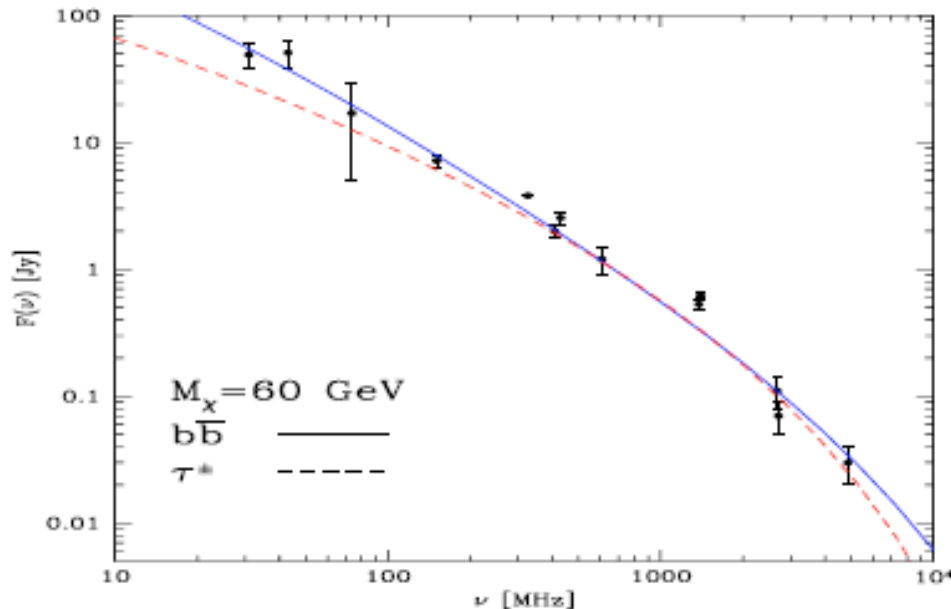
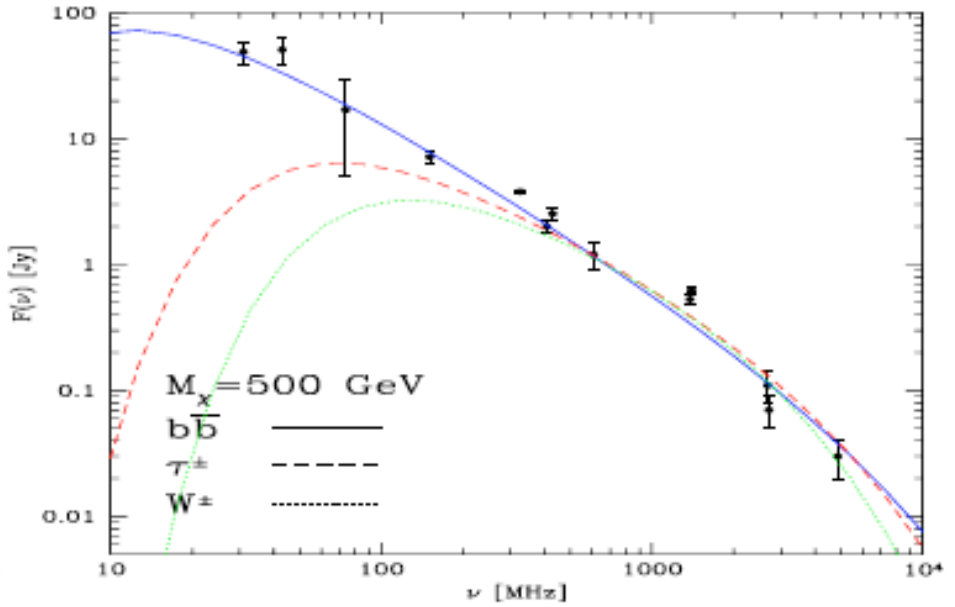
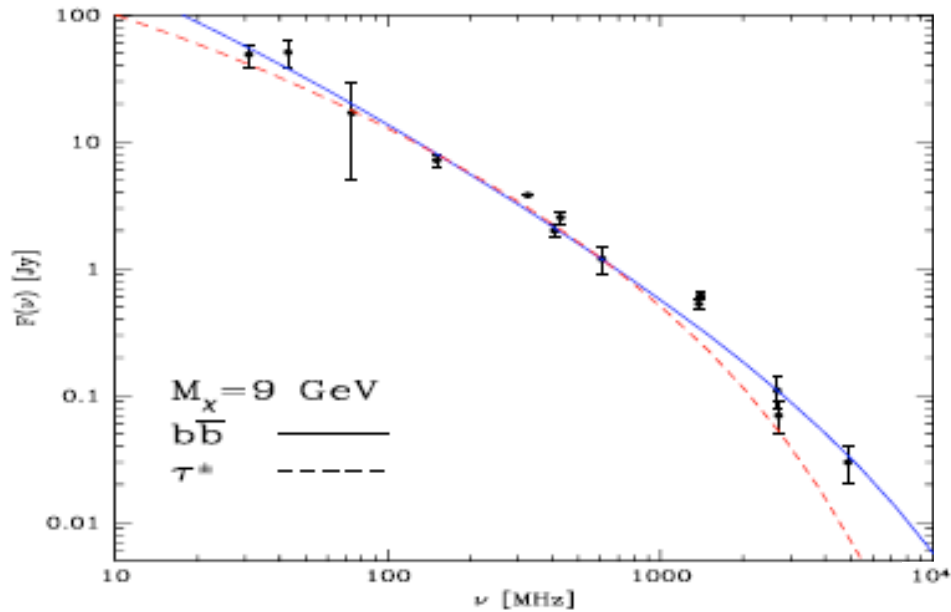
## 1<sup>st</sup> step:

Magnetic field and particle physics are left as free parameters to fit the radio halo of Coma

Compute electron equilibrium density

$$\frac{dn_e}{dE}(r, E) = \frac{1}{b(E)} \int_E^{M_x} dE' \hat{G}(r, \nu - \nu') Q_e(r, E')$$

# DM best fit to the radio halo spectrum of Coma



## 1<sup>st</sup> step:

Magnetic field and particle physics are left as free parameters to fit the radio halo of Coma

Compute synchrotron power,

$$P_{\text{synch}}(\nu, E, r) = \int_0^{\pi} d\theta \frac{\sin \theta}{2} 2\pi \sqrt{3} r_0 m c \nu_0 \sin \theta F(x / \sin \theta)$$

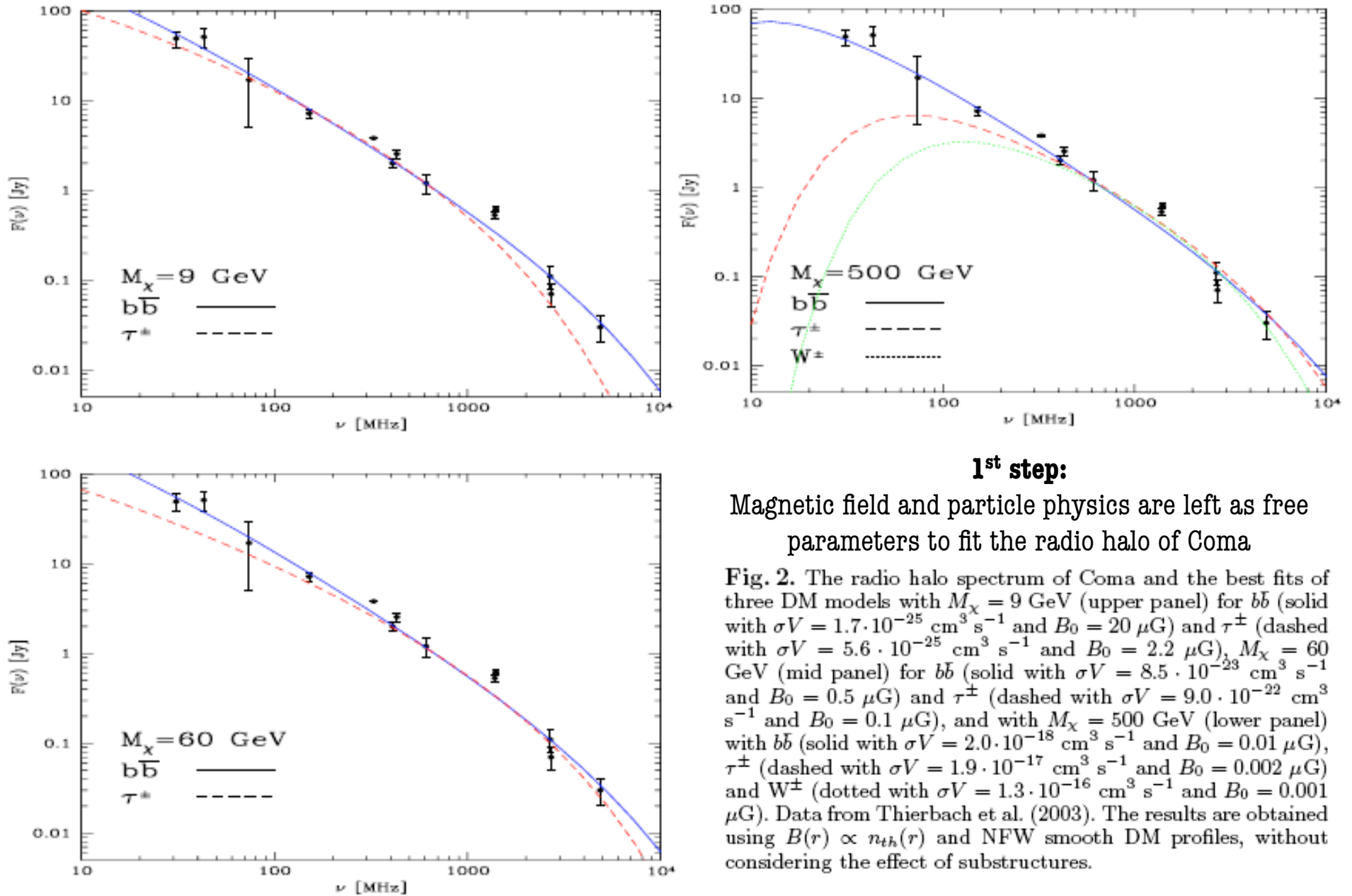
local emissivity

$$j_{\text{synch}}(\nu, r) = \int_{m_e}^{M_x} dE \left( \frac{dn_{e^-}}{dE} + \frac{dn_{e^+}}{dE} \right) P_{\text{synch}}(\nu, E, r)$$

and flux density spectrum

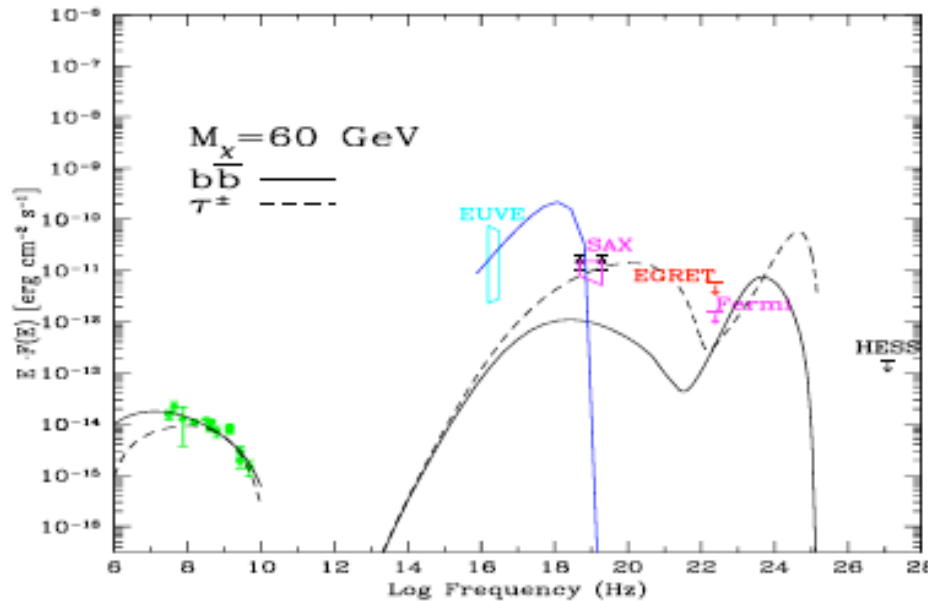
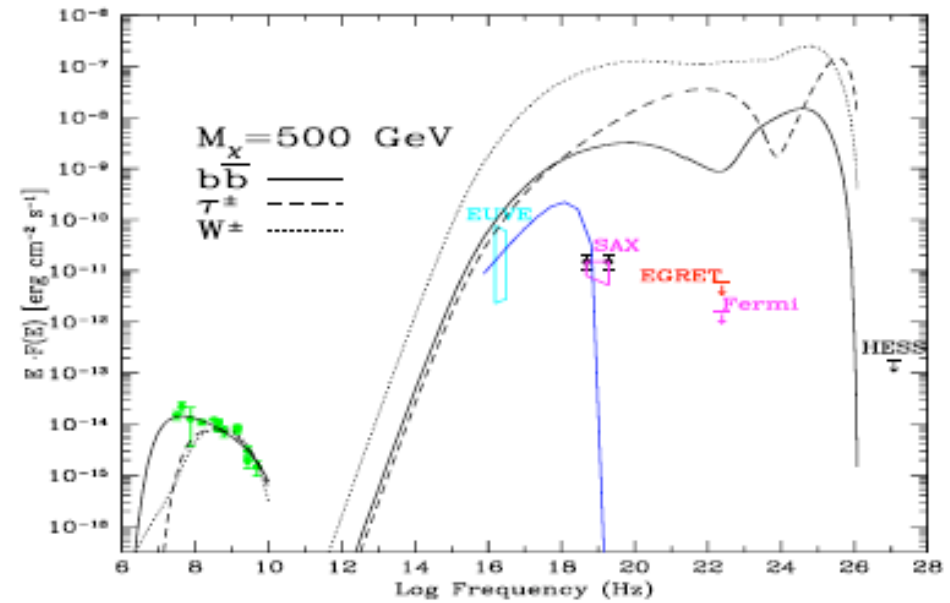
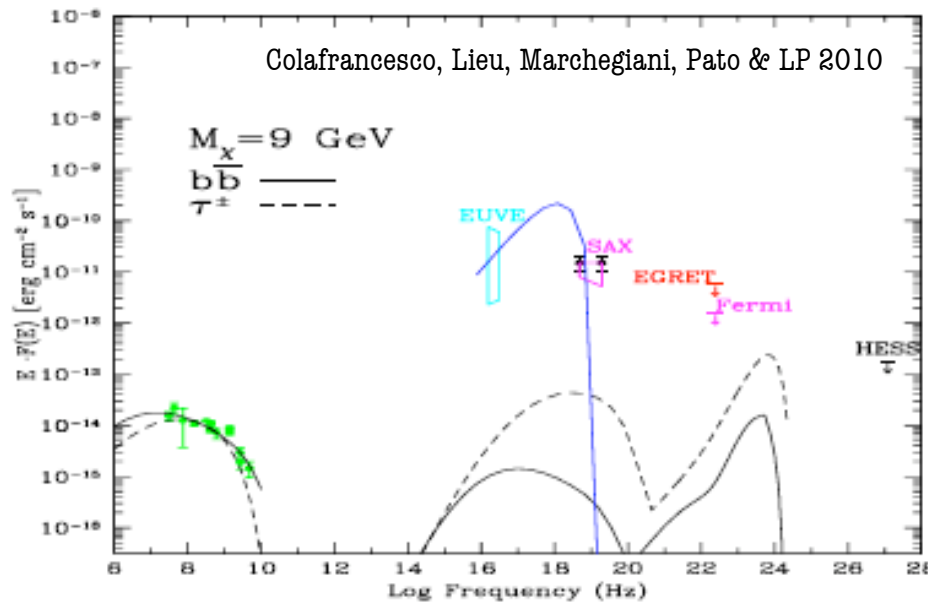
$$S_{\text{synch}}(\nu) = \int d^3 r \frac{j_{\text{synch}}(\nu, r)}{4\pi D_{\text{Coma}}^2}$$

# DM best fit to the radio halo spectrum of Coma





# Multiwavelength DM interpretation or exclusion?



## 2<sup>nd</sup> step:

The multiwavelength yield is compared with available measurements or upper limits

Compute Inverse Compton Scattering,

$$P_{\text{IC}}(E_\gamma, E) = c E_\gamma \int d\epsilon n(\epsilon) \sigma(E_\gamma, \epsilon, E)$$

$$j_{\text{IC}}(E_\gamma, r) = \int dE \left( \frac{dn_{e^-}}{dE} + \frac{dn_{e^+}}{dE} \right) P_{\text{IC}}(E_\gamma, E)$$

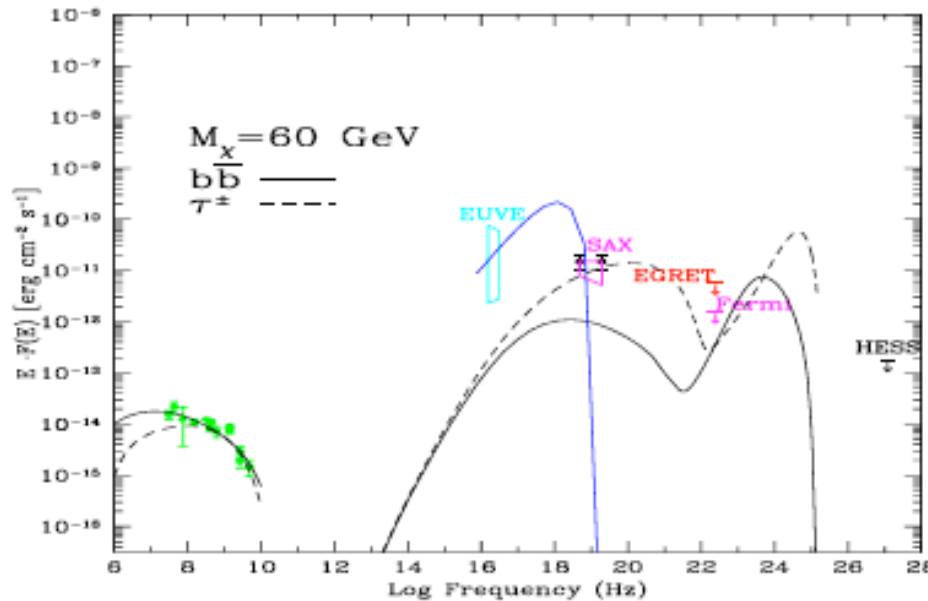
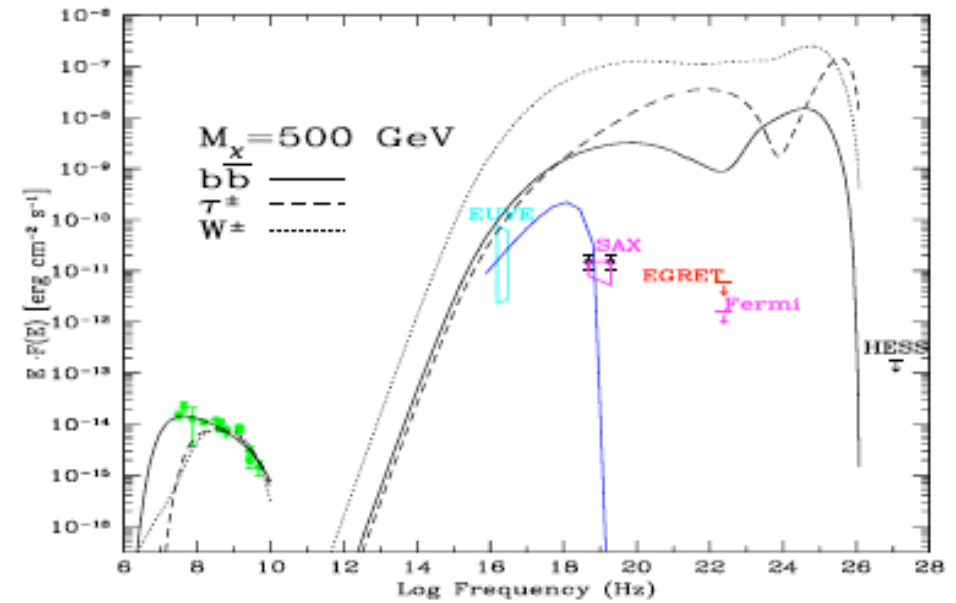
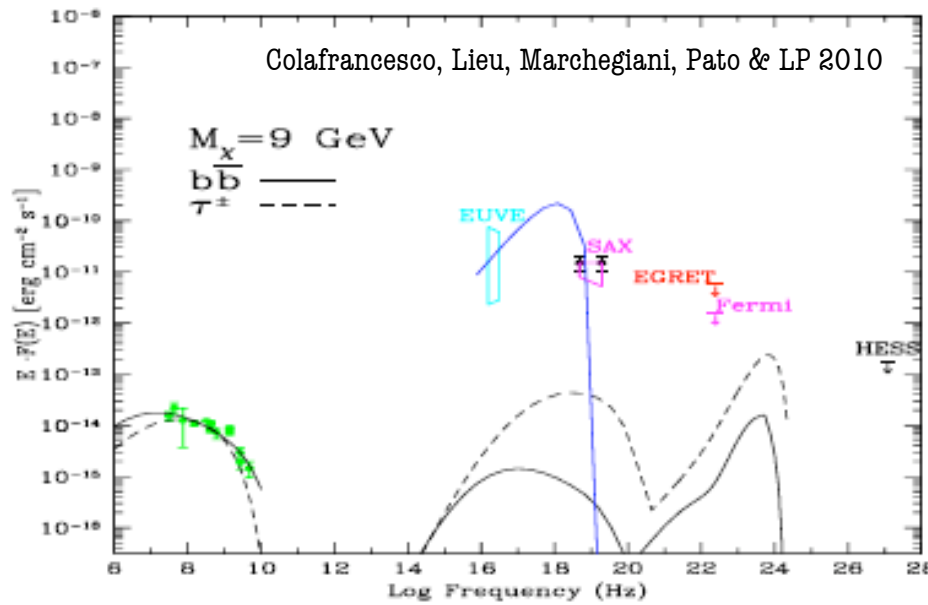
$$S_{\text{IC}}(E_\gamma) = \int d^3r \frac{j_{\text{IC}}(E_\gamma, r)}{4\pi D_{\text{Coma}}^2}$$

non-thermal bremsstrahlung

$$P_{\text{B}}(E_\gamma, E, r) = c E_\gamma \sum_j n_j(r) \sigma_j(E_\gamma, E)$$

and prompt  $\gamma$ -ray emission (more later)

# Multiwavelength DM interpretation or exclusion?

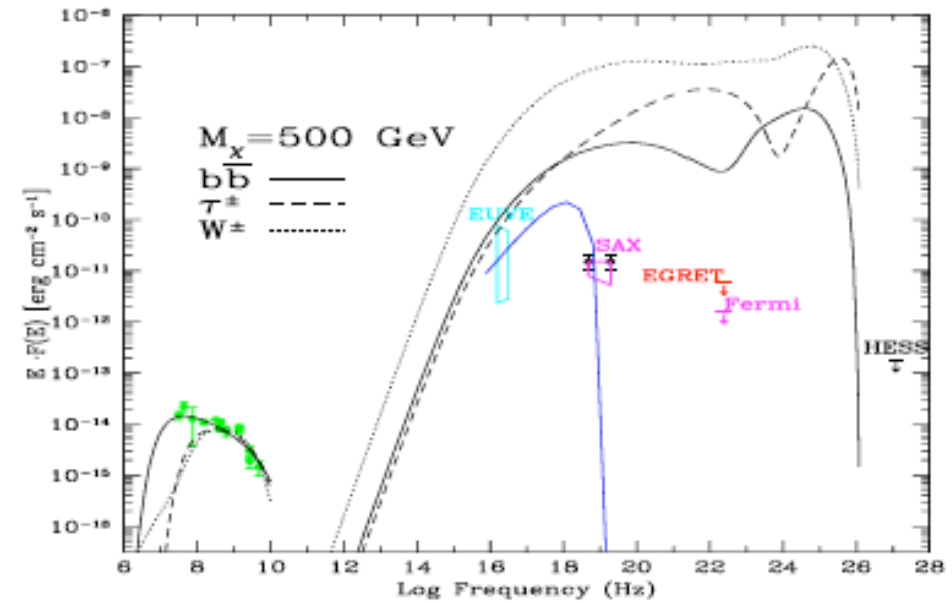
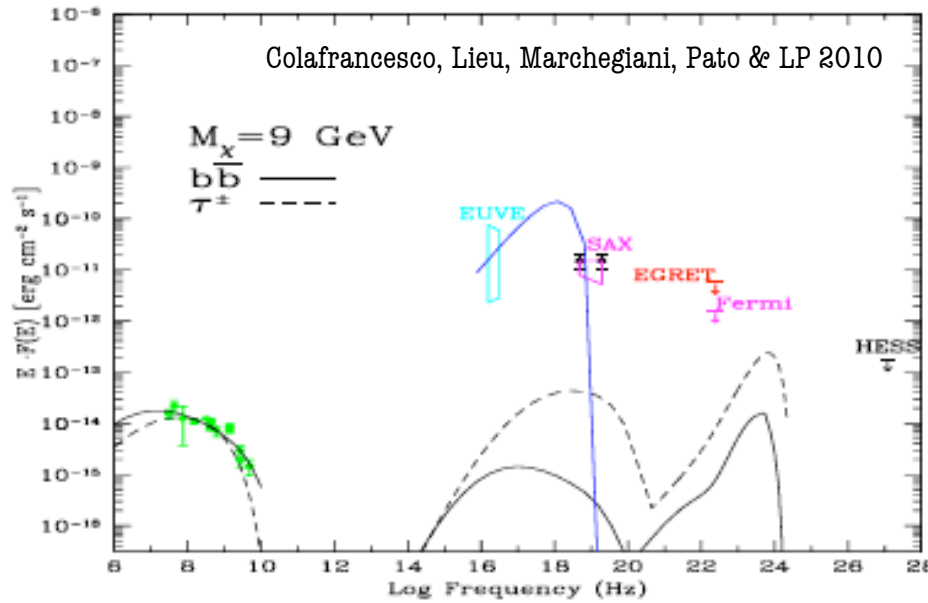


**2<sup>nd</sup> step:**

The multiwavelength yield is computed not to exceed other measurements

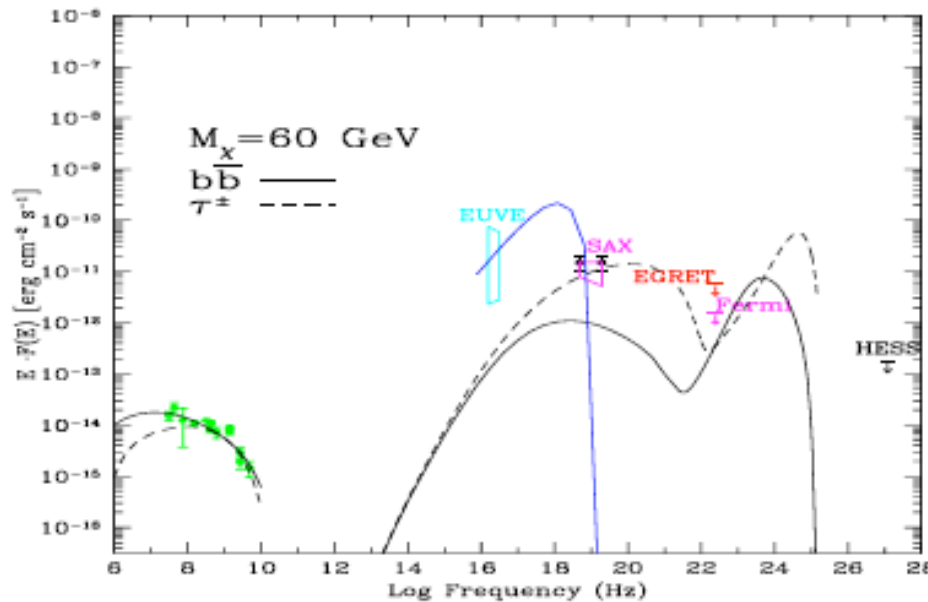
Fig. 4. The SED of the DM-induced e.m. signals in Coma as predicted by the three DM models. Upper panel:  $M_\chi = 9 \text{ GeV}$  (solid:  $b\bar{b}$ ; dashed:  $\tau^\pm$ ); mid panel:  $M_\chi = 60 \text{ GeV}$  (solid:  $b\bar{b}$ ; dashed:  $\tau^\pm$ ); lower panel:  $M_\chi = 500 \text{ GeV}$  (solid:  $b\bar{b}$ ; dashed:  $\tau^\pm$ ; dotted:  $W^\pm$ ) The values of  $\sigma V$  and  $B_0$  for the different models are the same used in Fig.2. The hatched regions in the X-ray domain represent data from PDS/BeppoSAX (Fusco-Femiano et al. 2004), HEXTE/RXTE (Rephaeli et al. 1999) and EUVE (Lieu et al. 1999). We also report the EGRET (Reimer et al 2003), Fermi (Mori 2009) and HESS (Aharonian et al. 2009a) upper limits on Coma. The blue line is a thermal bremsstrahlung model for Coma with  $kT = 8.2 \text{ keV}$  (Briel et al. 1992). The results are obtained using  $B(r) \propto n_{th}(r)$  and NFW smooth DM profiles, without considering the effect of substructures.

# Multiwavelength DM interpretation or exclusion?



**2<sup>nd</sup> step:**

The multiwavelength yield is computed not to exceed other measurements



No evidence for a combined explanation of non-thermal excesses in terms of Dark Matter annihilation



## Compatibility with the cluster heating rate

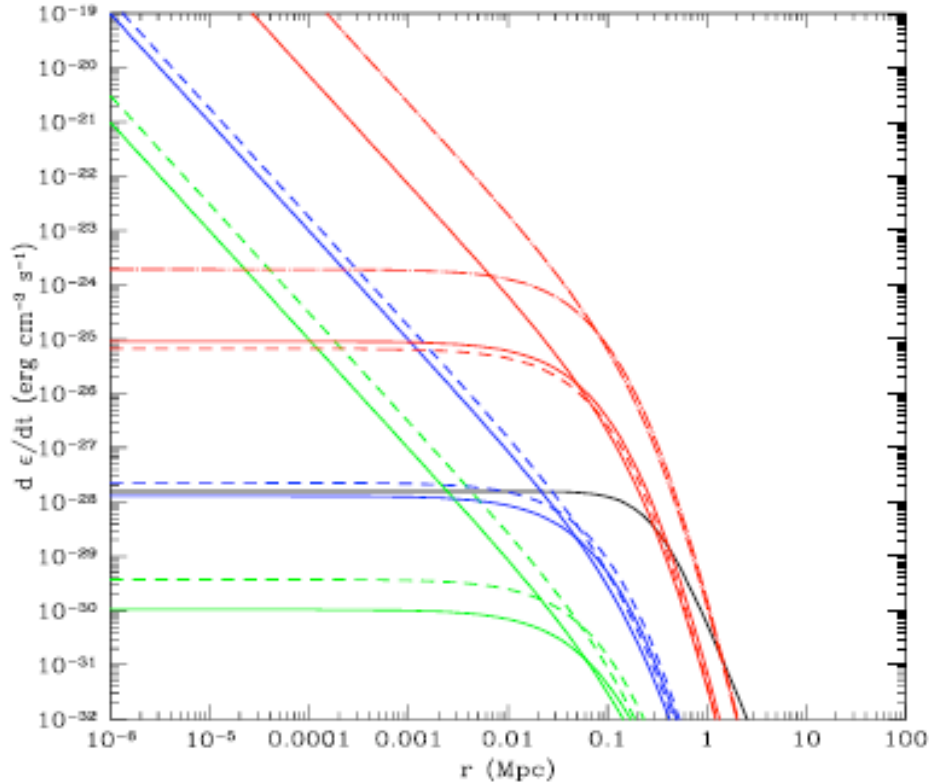


**Fig. 5.** The heating rate induced by DM secondary particles in Coma as predicted by the three DM models with  $M_\chi = 9$  GeV,  $M_\chi = 60$  GeV and  $M_\chi = 500$  GeV for  $b\bar{b}$  (solid),  $\tau^\pm$  (dashed),  $W^\pm$  (dot-dashed) compositions. We consider an NFW DM profile (green, blue and red peaking curves for 9, 60 and 500 GeV respectively) and a cored DM profile (green, blue and red flattening curves for 9, 60 and 500 GeV respectively). The values of  $\sigma V$  and  $B_0$  for the different models are the same used in Fig. 2. The solid black curve shows the bremsstrahlung cooling rate of the intra-cluster gas at a temperature of 8.2 keV. The results are obtained using  $B(r) \propto n_{th}(r)$  and smooth DM profiles, without considering the effect of substructures.

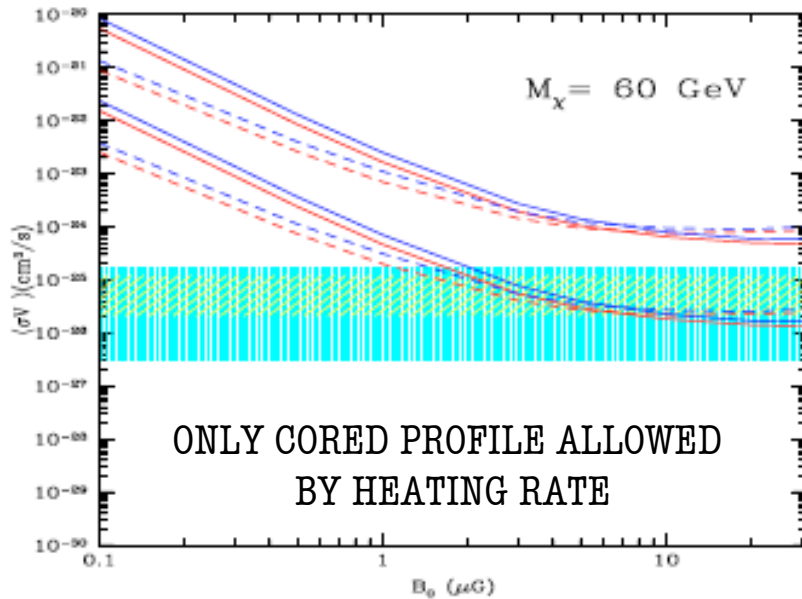
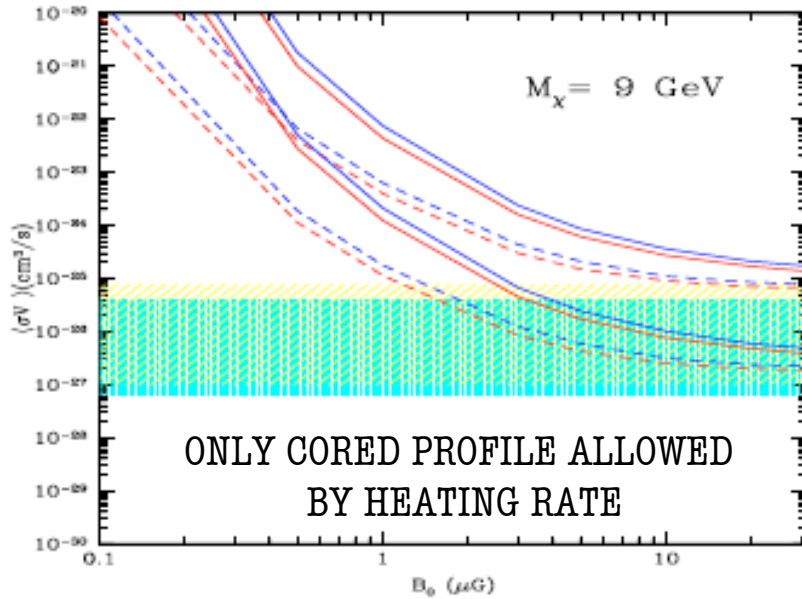
### 3<sup>rd</sup> step:

The heating rate of the intracluster gas due to Coulomb collision of low-energy non-thermal electrons should not exceed the bremsstrahlung cooling rate of thermal electrons

otherwise the heated gas would get a temperature higher than the one observed in the cluster, which is related to the cooling rate of thermal gas. We would observe a fast gas heating and expansion, while the cluster is thermally stable.

$$\frac{dE}{dt dV} = \int dE \frac{dn_e}{dE} \cdot \left( \frac{dE}{dt} \right)_{Coul}$$

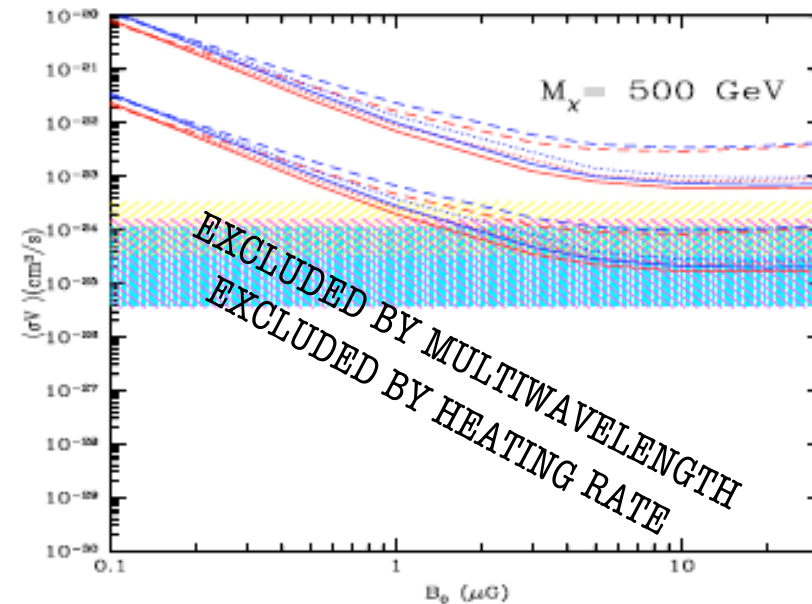
# Compatibility with multimessenger constraints



## 4<sup>th</sup> step (also called the killer step):

Cross-sections are compared with available constraints from GC  $\gamma$ s, diffuse  $\gamma$ s, antimatter, CMB, radio ... which excludes ANY dark matter interpretation for smooth profiles

Look at the upper curves: smooth cluster halo  
**All DM explanation are excluded**

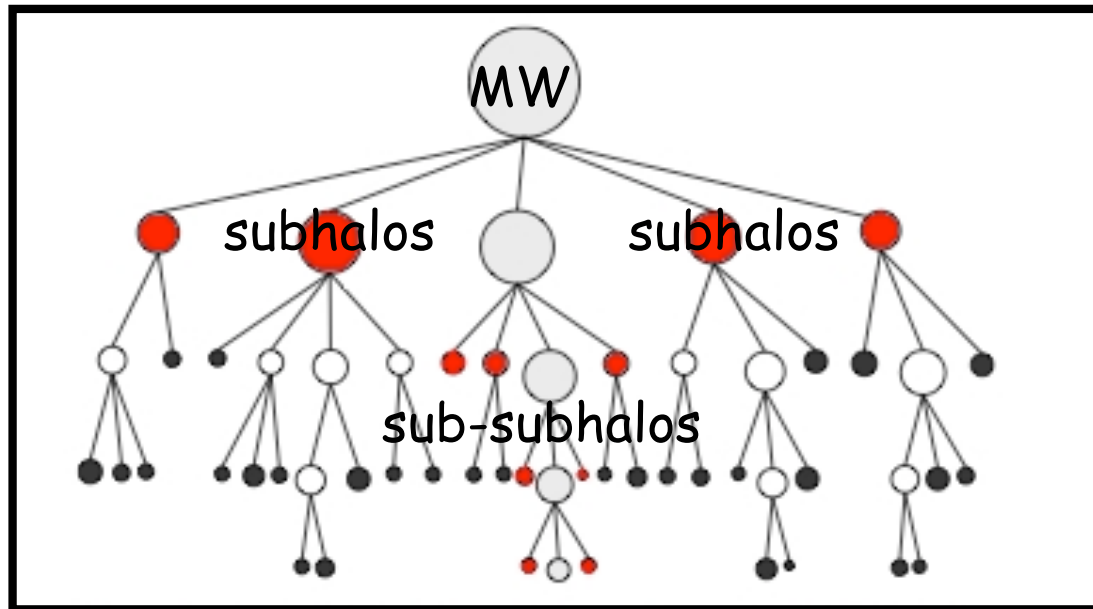


## Adding subhalos: modeling the structure of dark matter halos

Halos form through a hierarchical process of successive mergers.

The halo of our Galaxy will be self-similarly composed by:

- a smoothly distributed component ( $\rho_{\text{DM}(h)}^2$  single halo )
- a number of virialized substructures ( $\rho_{\text{DM}(\text{subh})}^2$  all halos)



Make use of simulations on galactic scale and use self-similarity arguments to infer cluster properties.

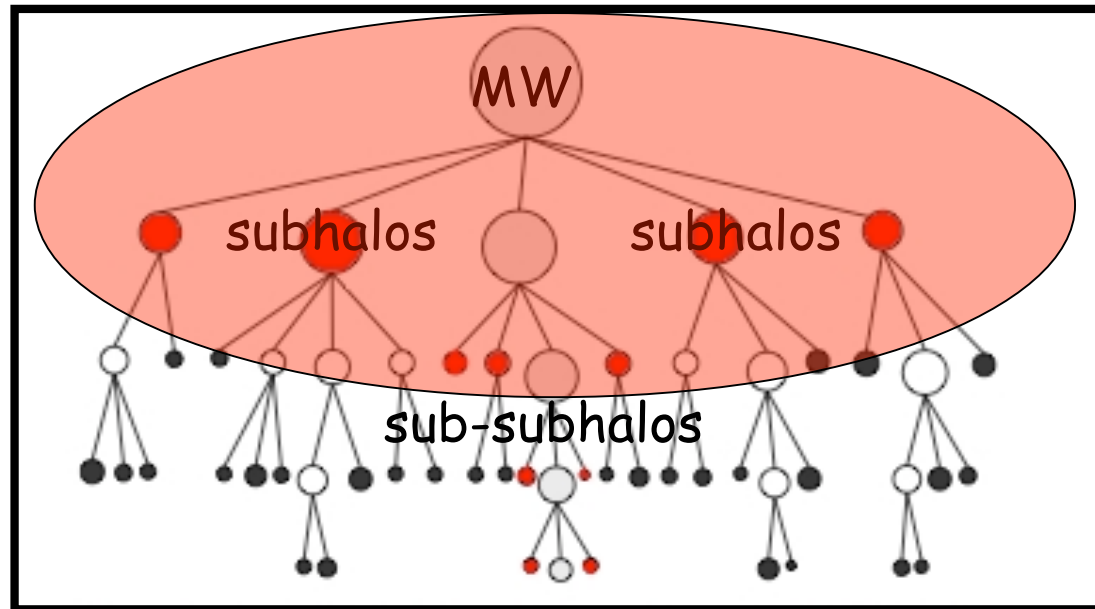
Note: self-similarity proven from cluster to galactic scale

# Adding subhalos: modeling the structure of dark matter halos

Halos form through a hierarchical process of successive mergers.

The halo of our Galaxy will be self-similarly composed by:

- a smoothly distributed component ( $\rho_{\text{DM}(h)}^2$  single halo )
- a number of virialized substructures ( $\rho_{\text{DM}(\text{subh})}^2$  all halos)



N-body simulations study the smooth halo and the larger halos ( $M > 10^5 M_{\text{sun}}$ ).

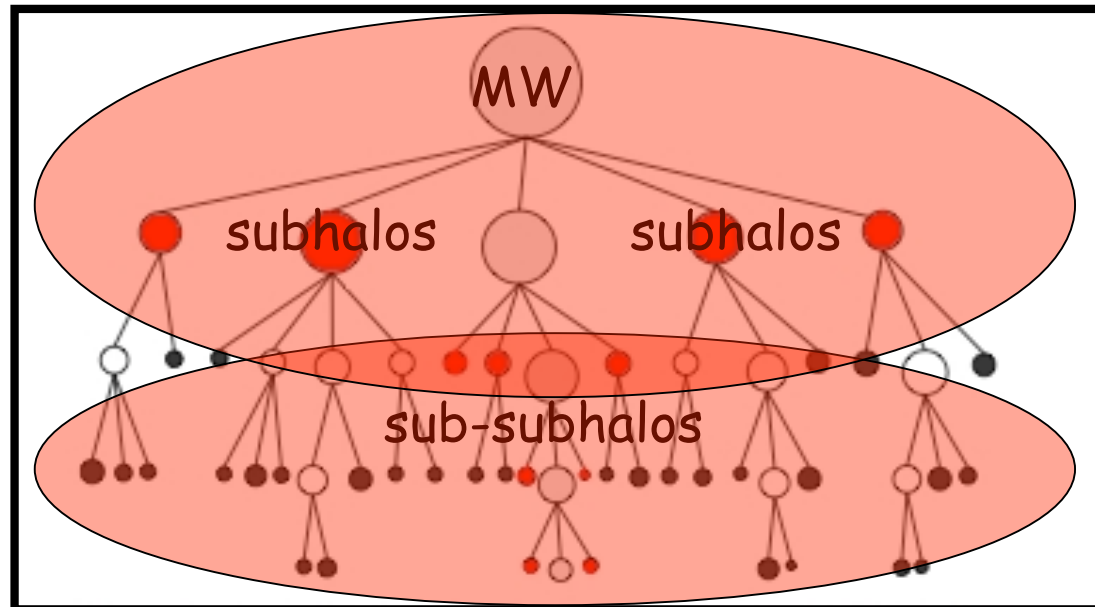


# Adding subhalos: modeling the structure of dark matter halos

Halos form through a hierarchical process of successive mergers.

The halo of our Galaxy will be self-similarly composed by:

- a smoothly distributed component ( $\rho_{\text{DM}(h)}^2$  single halo )
- a number of virialized substructures ( $\rho_{\text{DM}(\text{subh})}^2$  all halos)



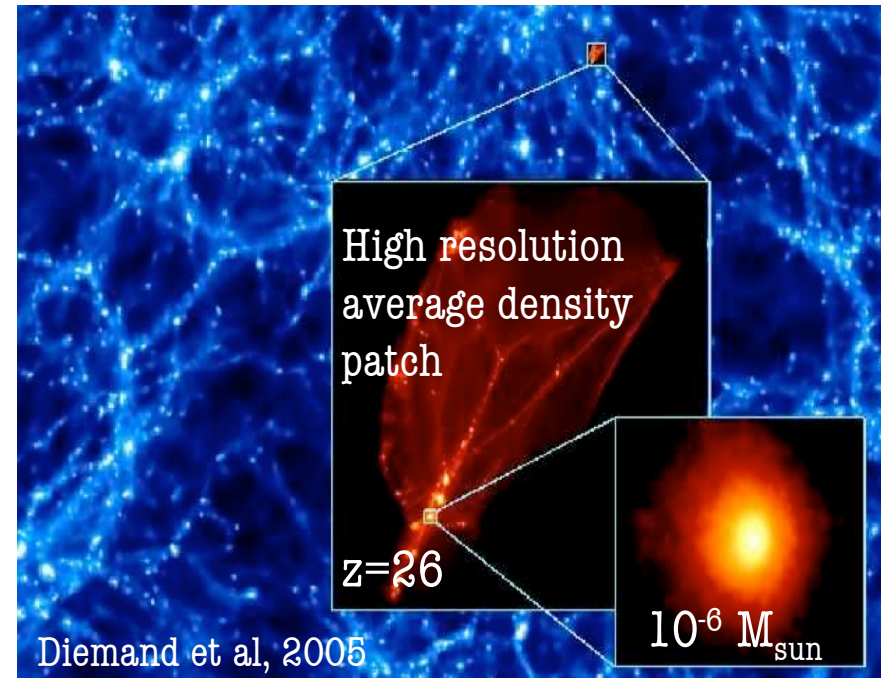
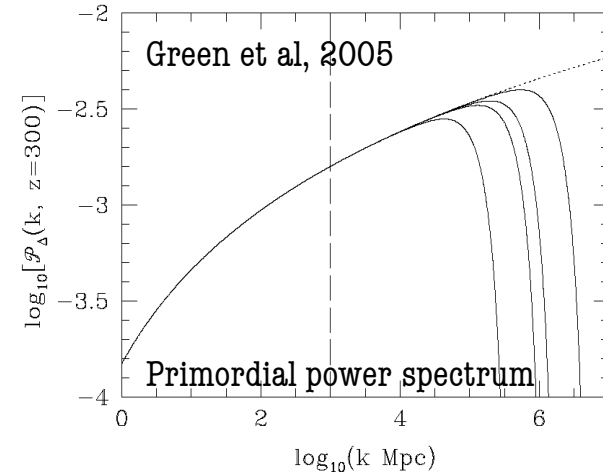
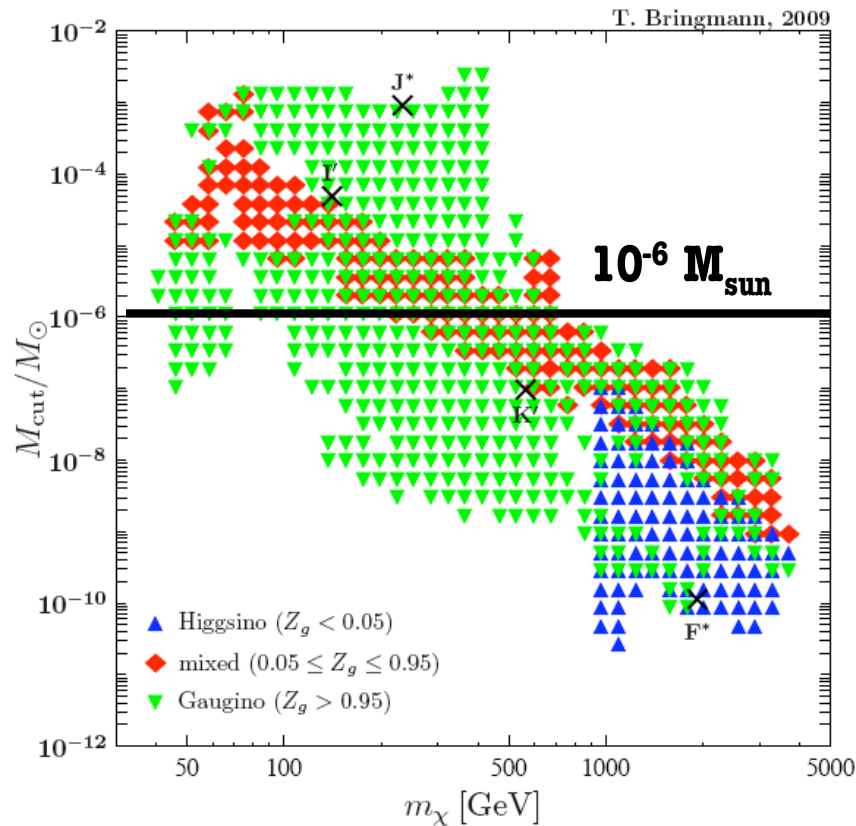
N-body simulations study the smooth halo and the larger halos ( $M > 10^5 M_{\text{sun}}$ ).

Microphysics and theory of structure formation sets the mass of the smallest halo because there is not enough CPU power to simulate small halos from collapse till today.

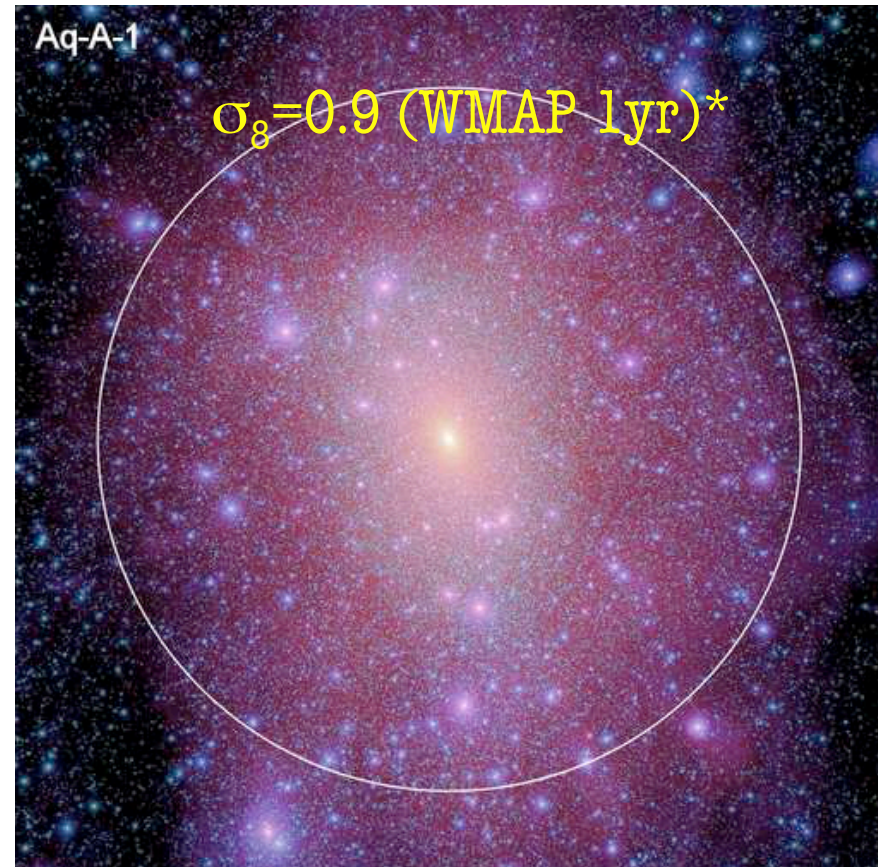
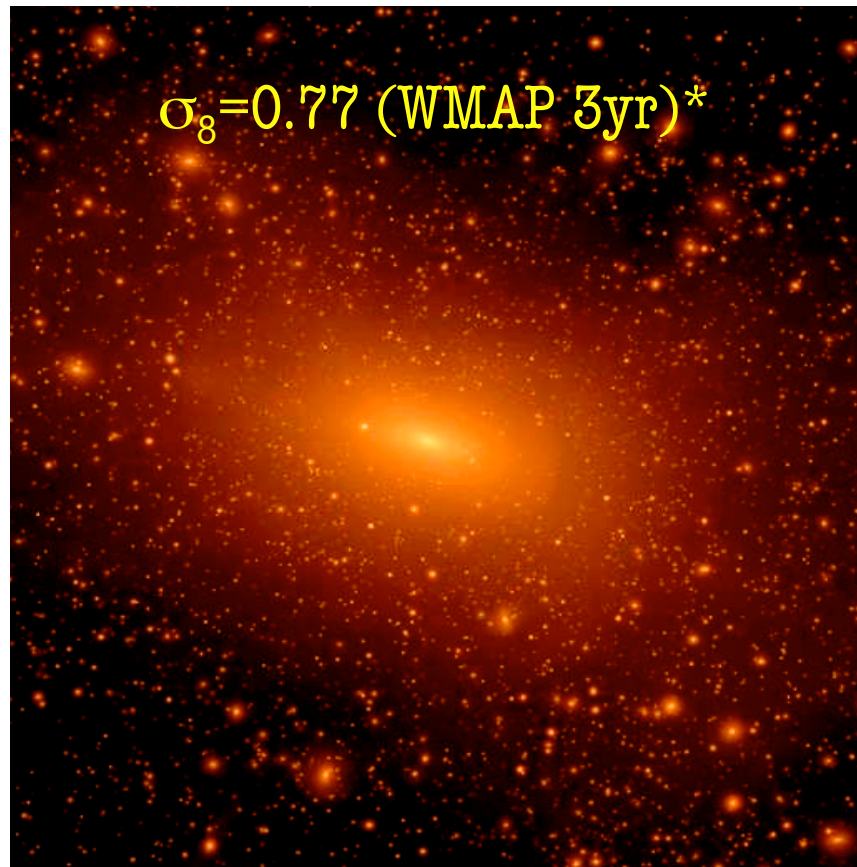
# Modeling the structure of dark matter halos from theory of structure formation ( $M < 10^5 M_{\text{sun}}$ )

**Theory:** Damping of the primordial power spectrum due to CDM free streaming or acoustic oscillations after kinetic decoupling

Typical  $M_{\text{min}}$  for a WIMP =  $10^{-6} M_{\text{sun}}$



Modeling the structure of dark matter halos  
from N-body simulations ( $M > 10^5 M_{\text{sun}}$ )



MW-like halos at  $z=0$

Via Lactea 2, Diemand et al

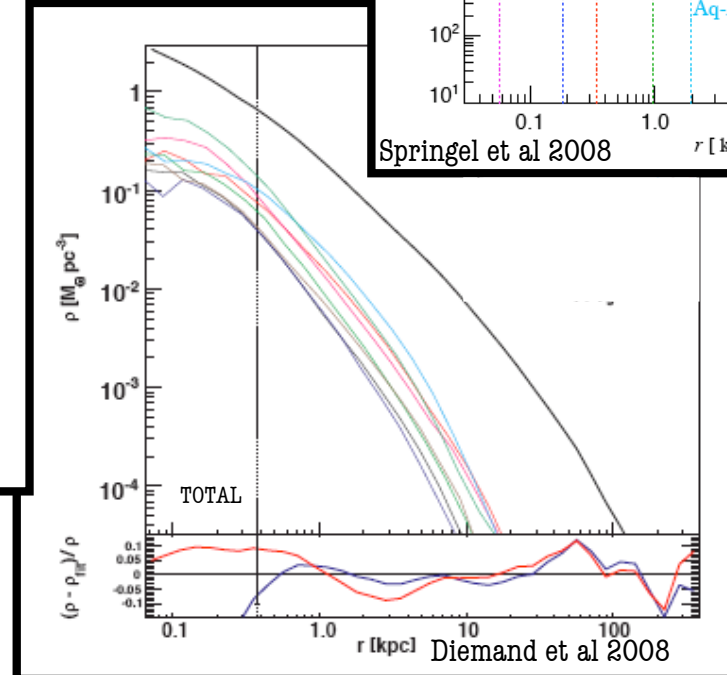
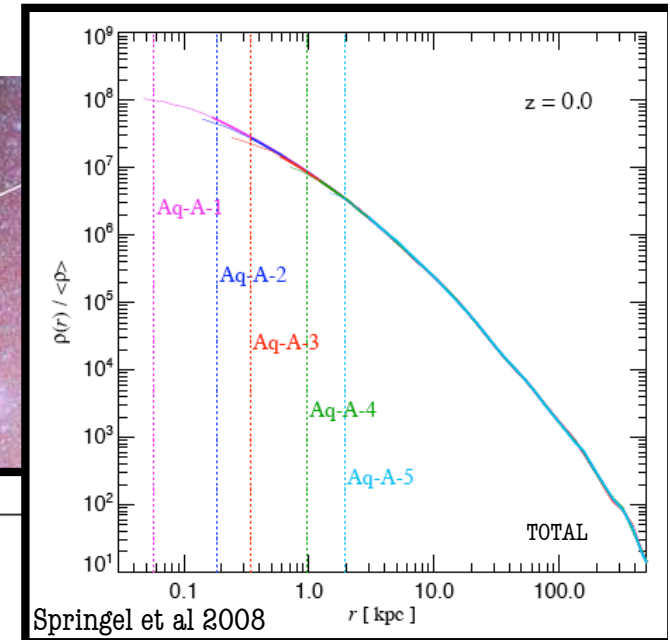
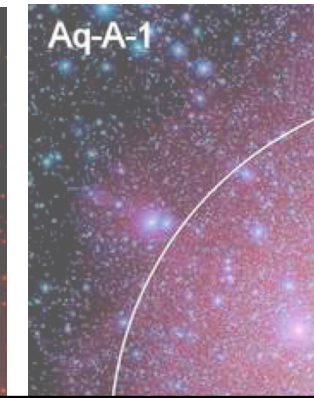
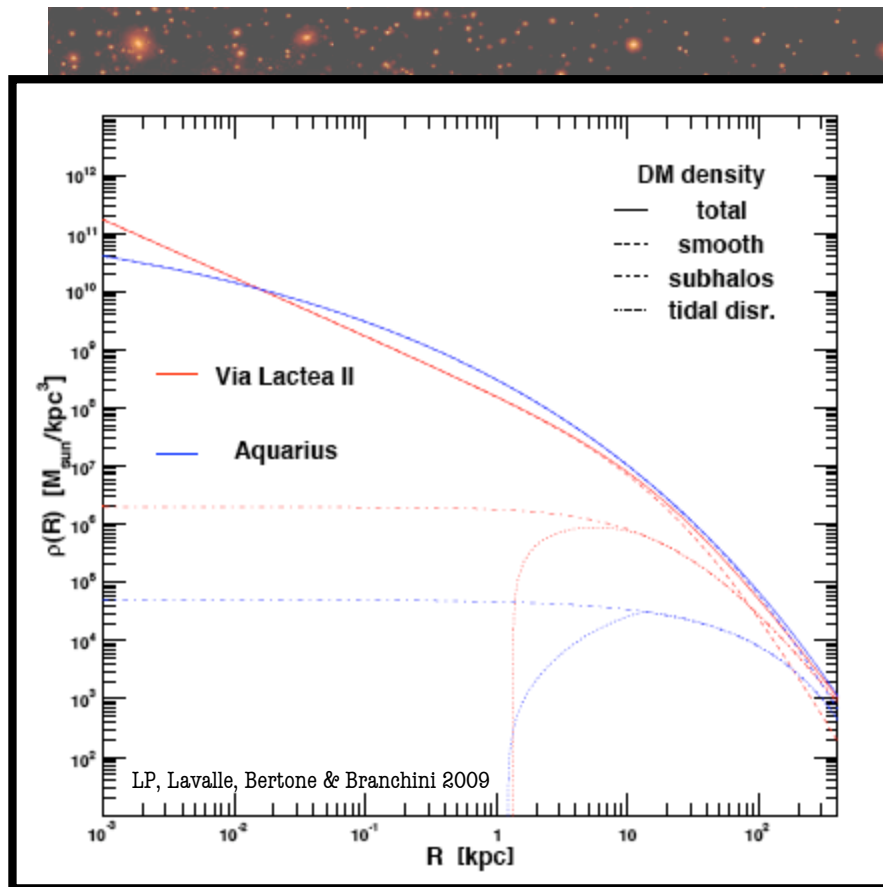
Aquarius, Springel et al

\*Note  $\sigma_8 = 0.8$  (WMAP 7yr)



# Modeling the structure of dark matter halos from N-body simulations ( $M > 10^5 M_{\text{sun}}$ )

## Halo and subhalo profile shape



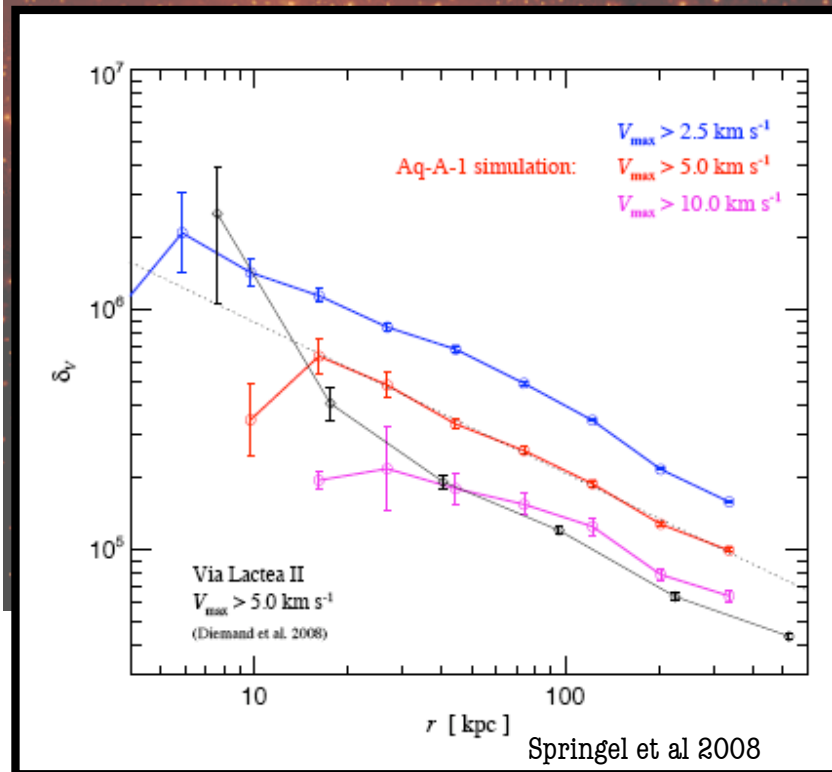
Warning: NFW or Einasto are total profiles (smooth + subhalo)



# Modeling the structure of dark matter halos from N-body simulations ( $M > 10^5 M_{\text{sun}}$ )

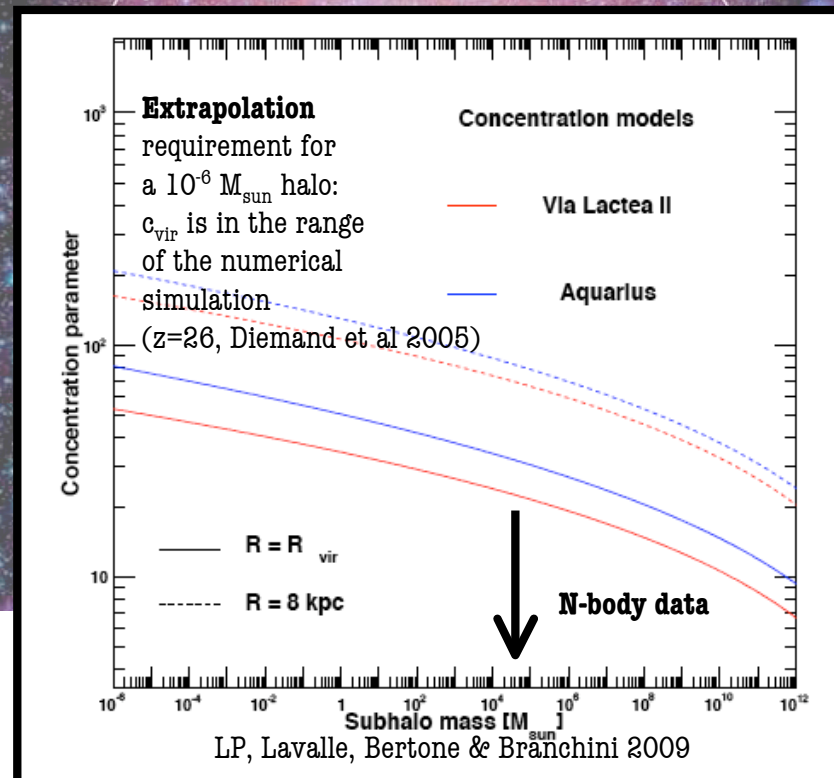
## Halo and subhalo profile shape and concentration

Concentration parameter  
differ (because of  $\sigma_8$ )



Aq-A-1

Concentration parameter  
( $R_{\text{vir}}/r_s$ ) has radial dependence  
higher concentration  $\rightarrow$  higher flux!



Modeling the structure of dark matter halos  
 from N-body simulations ( $M > 10^5 M_{\text{sun}}$ )

**Halo and subhalo profile shape and concentration**

Concentration parameter  
 differ (because of  $\sigma_8$ )

Aq-A-1

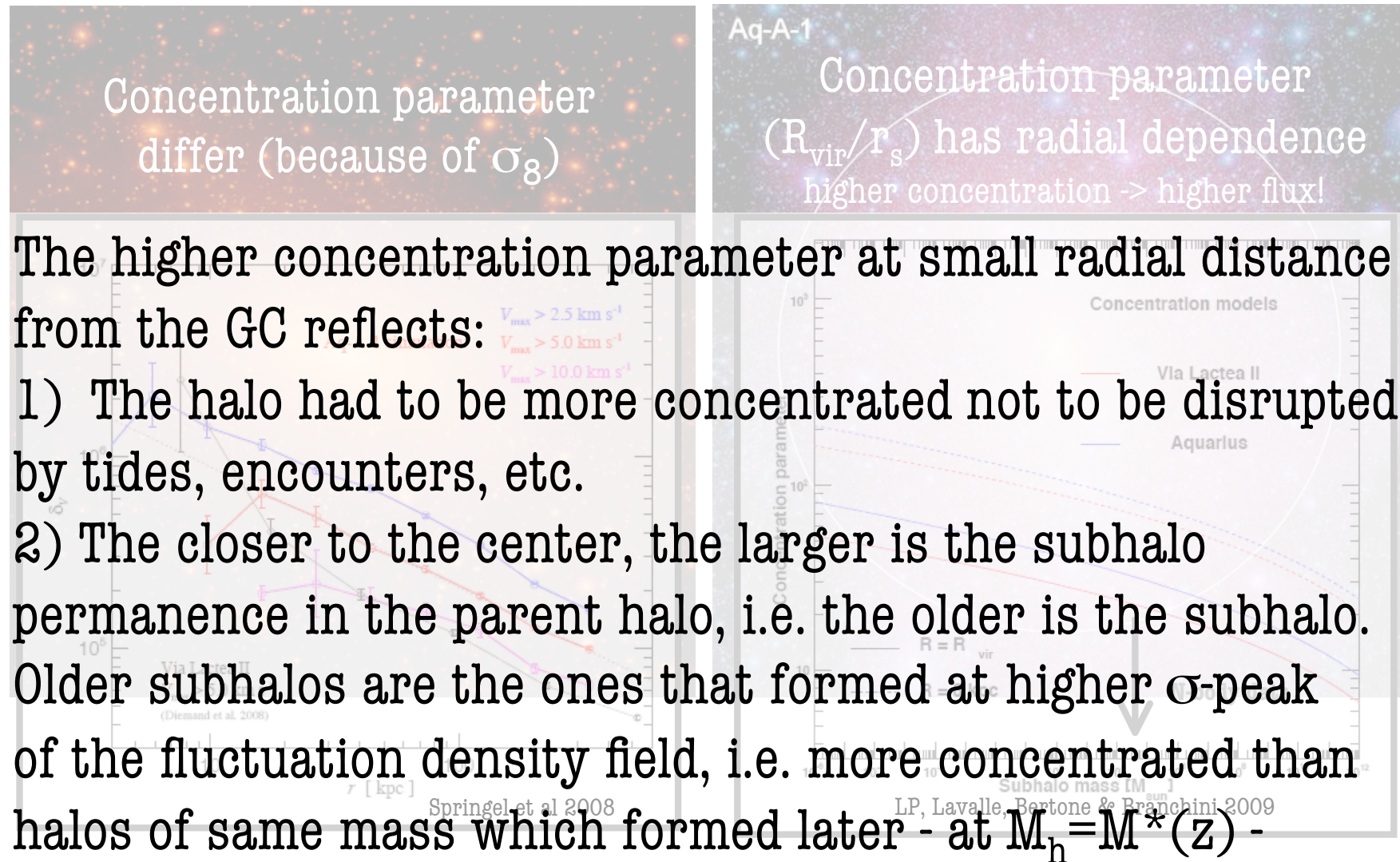
Concentration parameter  
 $(R_{\text{vir}}/r_s)$  has radial dependence  
 higher concentration  $\rightarrow$  higher flux!

The higher concentration parameter at small radial distance from the GC reflects:

1) The halo had to be more concentrated not to be disrupted by tides, encounters, etc.

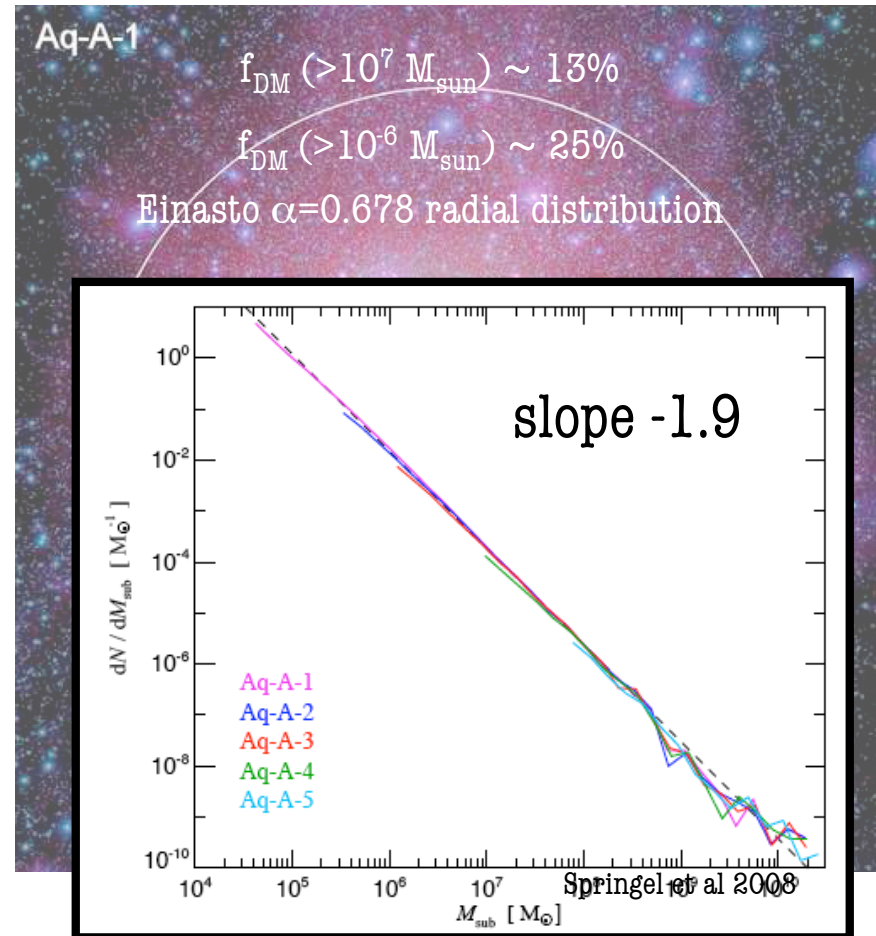
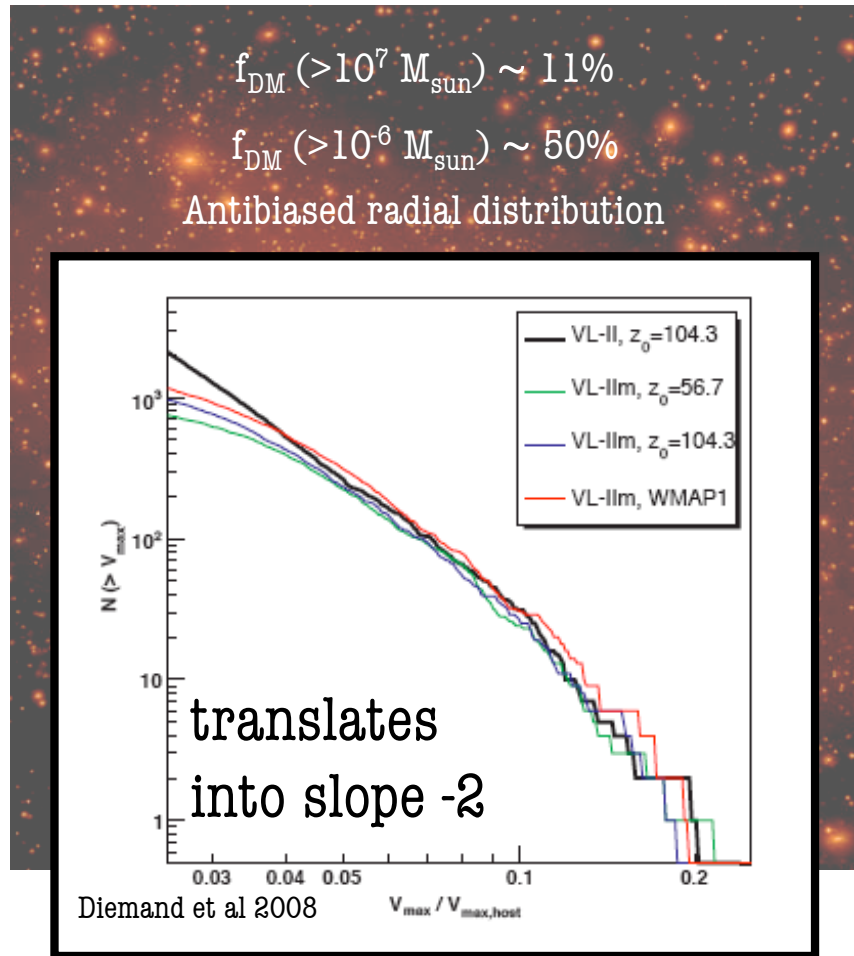
2) The closer to the center, the larger is the subhalo permanence in the parent halo, i.e. the older is the subhalo. Older subhalos are the ones that formed at higher  $\sigma$ -peak of the fluctuation density field, i.e. more concentrated than

halos of same mass which formed later - at  $M_h = M^*(z)$  -



# Modeling the structure of dark matter halos from N-body simulations ( $M > 10^5 M_{\text{sun}}$ )

## Subhalo abundance and density distribution

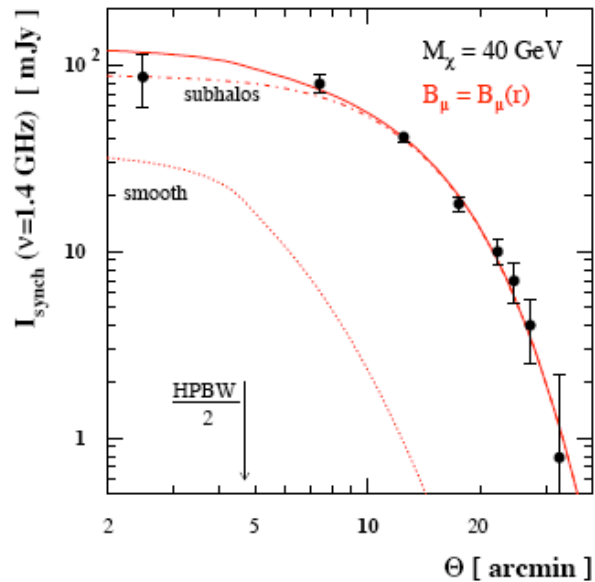
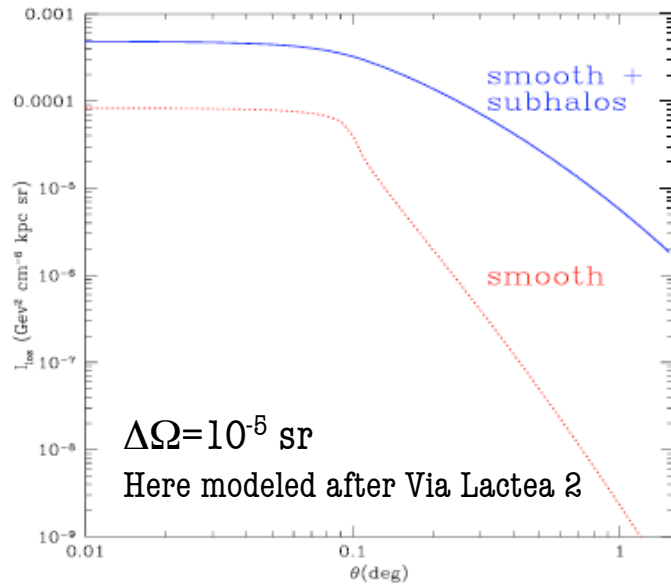


Note the different subhalo definition ( $v_{\text{max}}$  VS mass)  
 Slope -1.95 is consistent with both simulations within the fit errors



# Compatibility with multimessenger constraints adding subhalos

Colafrancesco, Lieu, Marchegiani, Pato & LP 2010

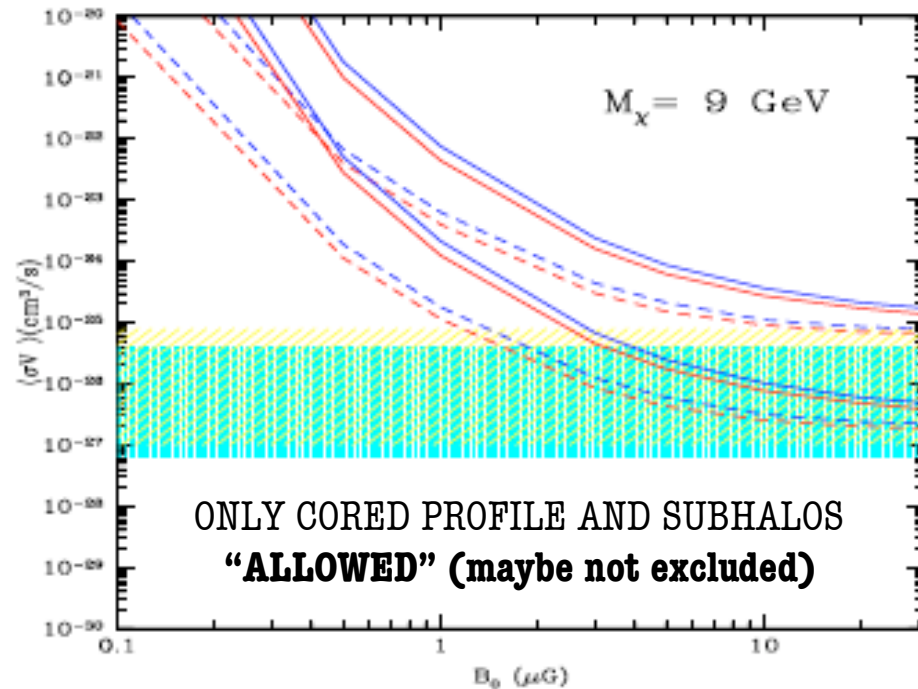


Colafrancesco, Profumo & Ullio 2006

## Subhalo population

In presence of a population of substructures with  $M_{\min} = 10^{-6} M_{\text{sun}}$  and radial dependence of the concentration parameter, a boost of  $\sim 35$  still let some models allowed, providing a favourable environment (MW DM structure and propagation model)

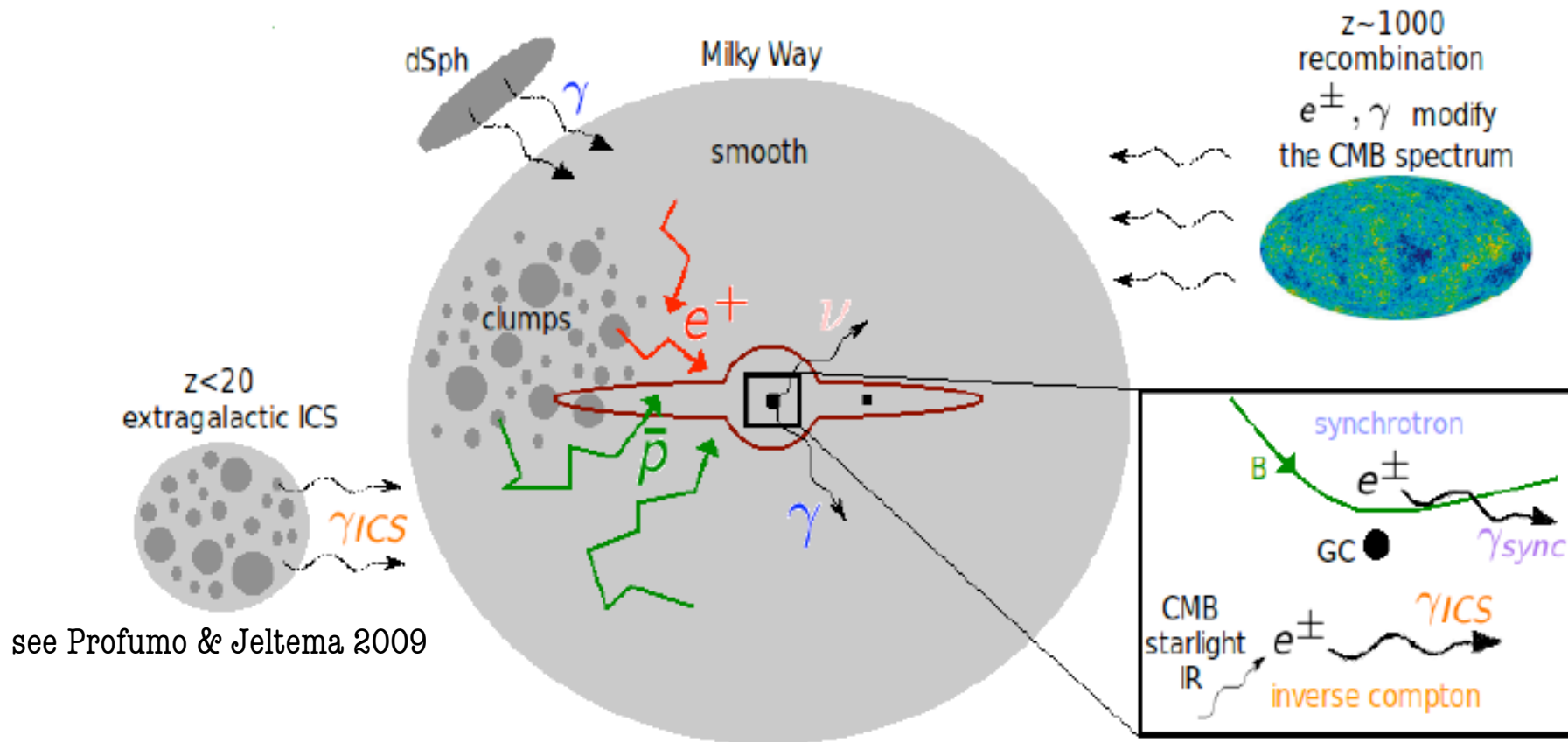
Note that subhalos are also needed to explain the surface brightness profile of the radio halo





# The multiwavelength/multimessenger/multi-target approach

$$\Phi = \text{ParticlePhysics} \times \text{Cosmology/Astrophysics} \times \text{Transport}$$



## The $\gamma$ -ray sky

$$\Phi_\gamma = \Phi_{\text{particle physics}} \times \Phi_{\text{cosmology}}$$

### MW smooth and single subhalo contribution

$$\Phi_{\text{COSMO}}^{\text{halo}}(M, R, r) \propto \int_{\text{l.o.s.}} d\lambda d\Omega \left[ \frac{\rho_{\text{DM}}^2(M, c(M, R), r, \psi)}{d^2} \right]$$

### Integrated contribution of all the GALACTIC halos along the LOS

$$\Phi^{\text{allhalos}}_{\text{COSMO}}(\psi, \Delta\Omega) \propto \int_M dM \int_c dc \iint_{\Delta\Omega} d\vartheta d\varphi \int_{\text{l.o.s.}} d\lambda \rho_{\text{sh}}(M, R) \cdot P(c) \Phi_{\text{COSMO}}^{\text{halo}}$$

### Integrated contribution of EXTRAGALACTIC halos and subhalos

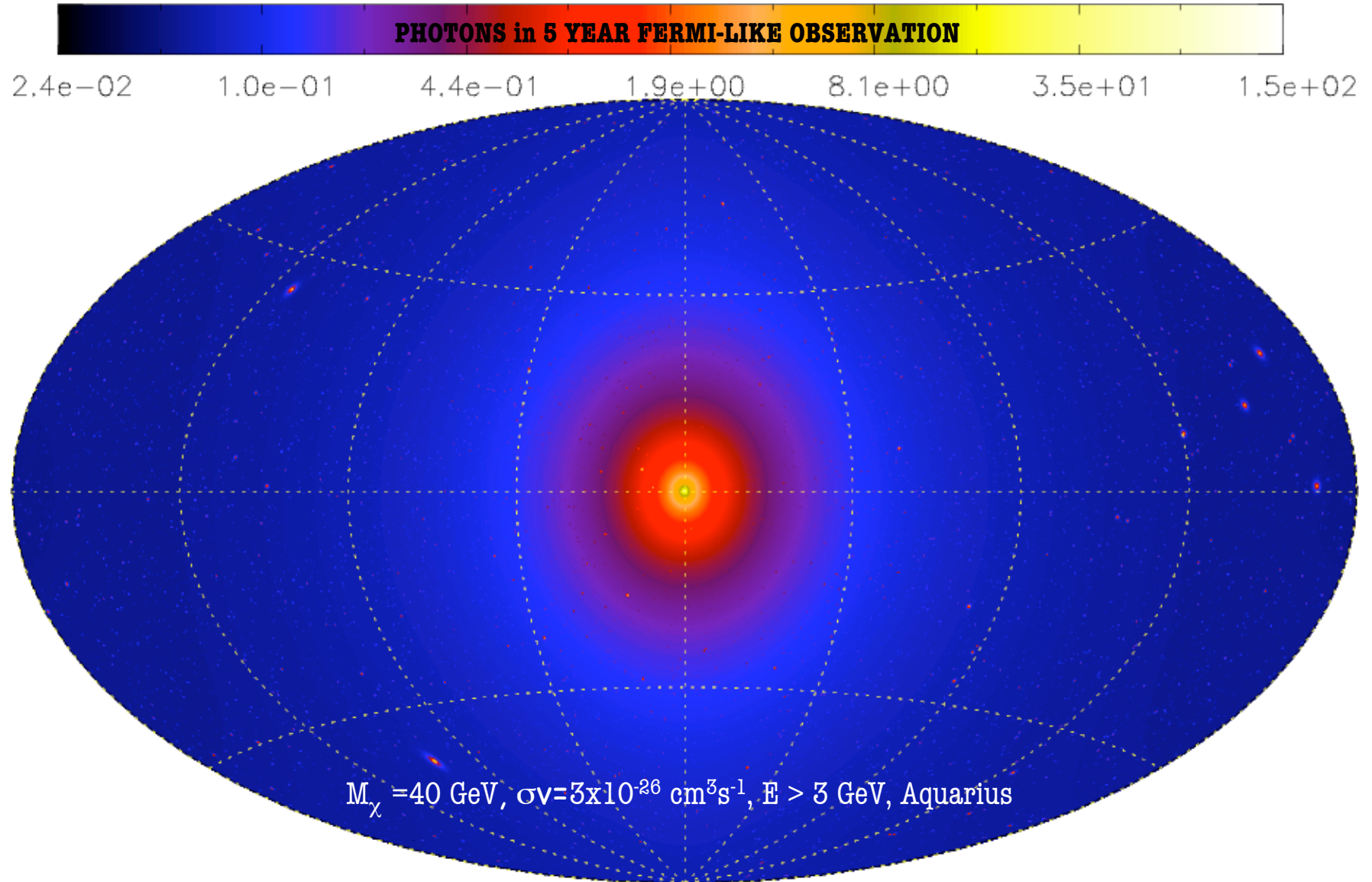
Computing the cosmological  $\gamma$ -ray flux due to DM annihilation in halos and subhalos

$$\frac{d\phi_\gamma}{dE_0} = \frac{\sigma v}{8\pi} \frac{c}{H_0} \frac{\bar{\rho}_0^2}{m_\chi^2} \int dz (1+z)^3 \frac{\Delta^2(z)}{h(z)} \frac{dN_\gamma(E_0(1+z))}{dE} e^{-\tau(z, E_0)}$$

Enhancement due to halo weighted for the halo and subhalo mass function
 $\propto \frac{d\log N}{d\log M} \Phi_{\text{COSMO}}^{\text{halo}}$

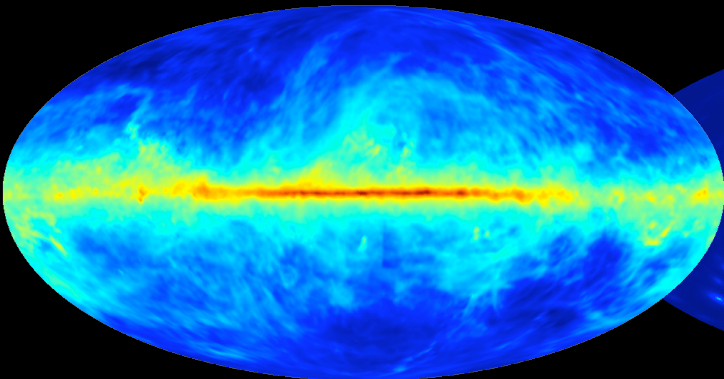
# The $\gamma$ -ray sky

## Galactic and extragalactic: smooth + subhalos

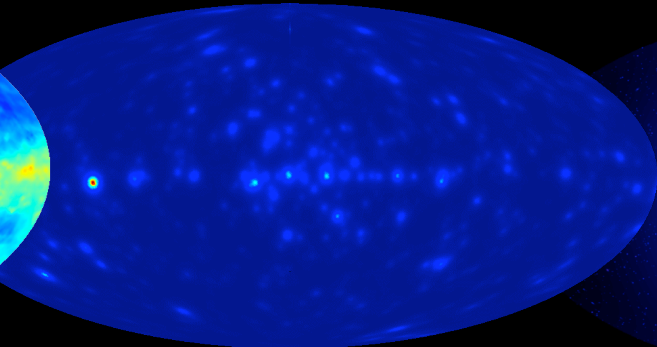


to be compared with the available data after background subtraction

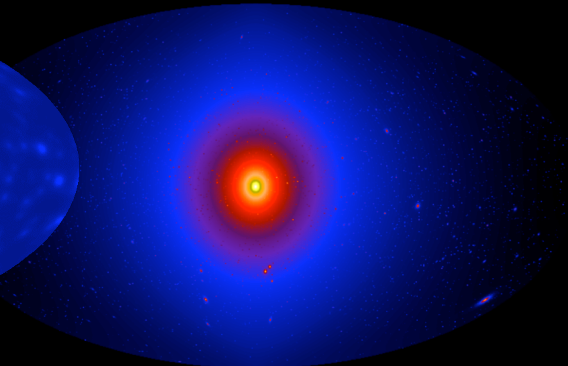
ingredients



galactic diffuse model (+ isotropic)

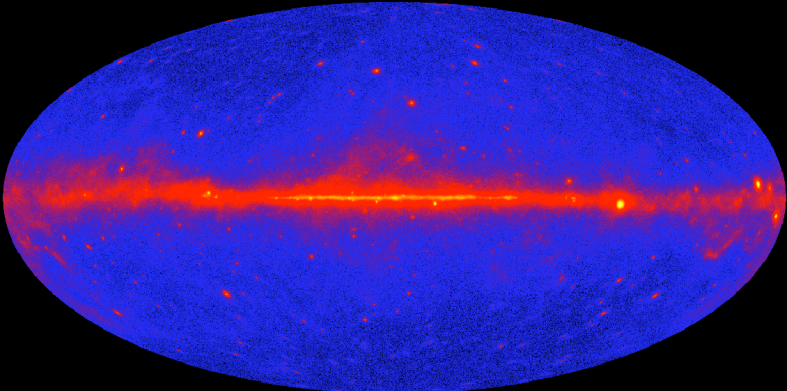


point sources data

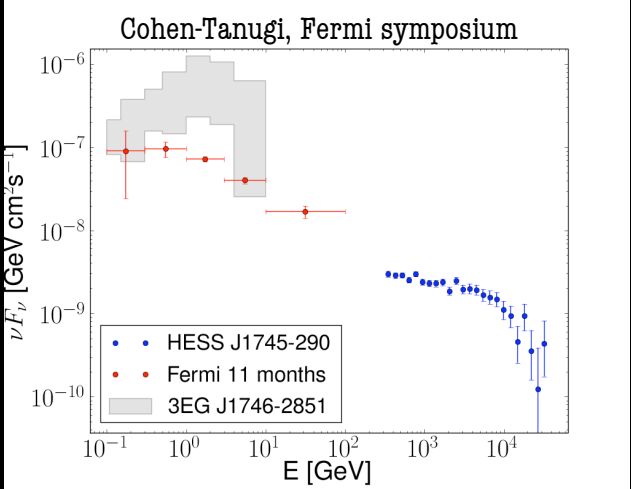


dark matter model

data



Fermi data



Galactic Center data



# The antimatter sky - coherent halo description wrt $\gamma$ -rays

Compute the number density à la Delahaye et al. 2008

$$n_{CR}(t, \bar{x}, E_{CR}) \equiv \frac{d^2 N_{CR}}{dV dE_{CR}}$$

electrons and positrons

$$\frac{\partial n_{e^+}}{\partial t} - \underbrace{K_{e^+}(E_{e^+}) \nabla^2 n_{e^+}}_{\text{diffusion (cilindric)}} - \underbrace{\frac{\partial}{\partial E_{e^+}} (b(E_{e^+}) n_{e^+})}_{\text{losses: ICS + synchrotron}} = \underbrace{Q_{e^+}(\bar{x}, E_{e^+})}_{\text{source term}}$$

protons and antiprotons

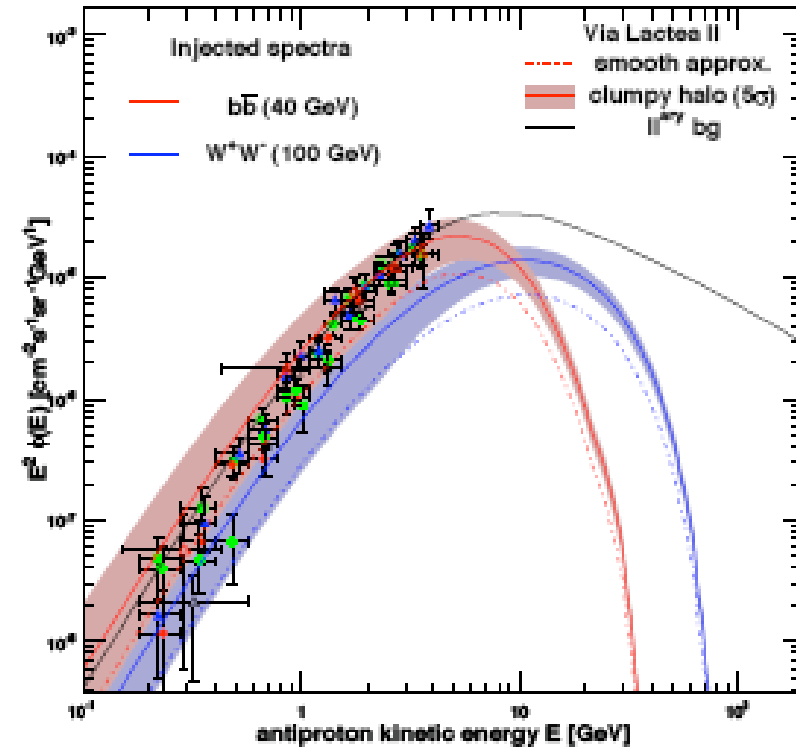
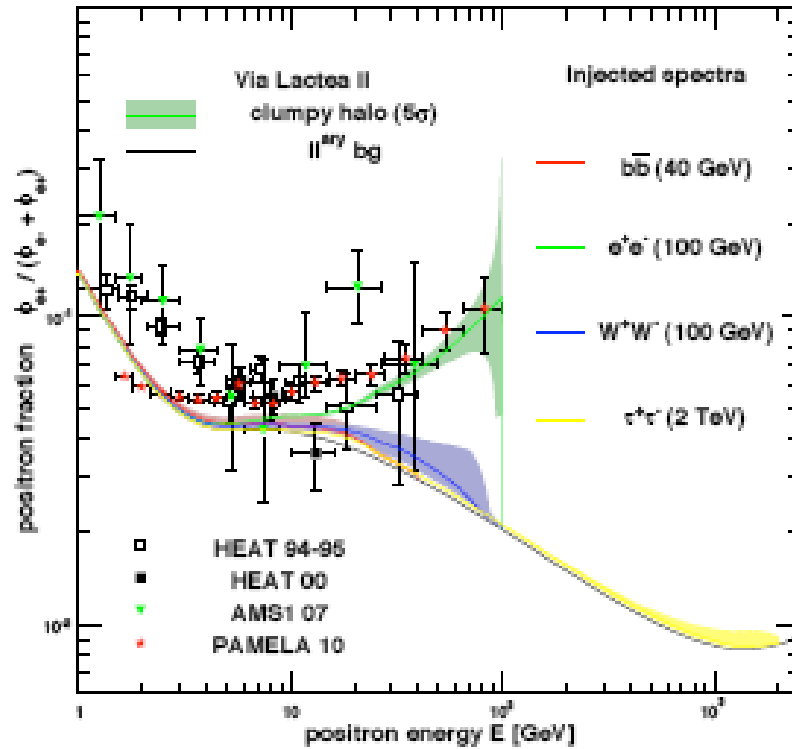
$$\frac{\partial n_{\bar{p}}}{\partial t} - K_{\bar{p}}(T_{\bar{p}}) \nabla^2 n_{\bar{p}} - \frac{\partial}{\partial z} (\underbrace{\text{sgn}(z) V_c}_{\text{galactic winds}} n_{\bar{p}}) = Q_{\bar{p}}(\bar{x}, T_{\bar{p}}) - \underbrace{2h \delta_D(z) \Gamma_{\text{ann}}^{p\bar{p}}(T_{\bar{p}})}_{\text{destruction in the disk}} n_{\bar{p}}$$

Compute fluxes and boosts à la Lavalley et al. 2008

$$\phi_{CR,sm}(E_{CR}) \propto \langle \sigma v \rangle \int_{E_{CR}}^{\infty} dE \frac{dN_{CR}}{dE} \int_{\text{diff.zone}} d^3 \bar{x} \left( \frac{\rho_{sm}(\bar{x})}{\rho_{sun}} \right)^2 G_{sun}^{CR}(\bar{x}, \lambda_D)$$

$$\langle \phi_{CR,cl} \rangle (E_{CR}) \propto \langle \sigma v \rangle N_{cl} \int_{E_{CR}}^{\infty} dE \frac{dN_{CR}}{dE} \int_{\text{diff.zone}} d^3 \bar{x} \langle \xi \rangle_M(R) \frac{dP_V}{dV}(R) G_{sun}^{CR}(\bar{x}, \lambda_D) = N_{tot}^{sub} \langle \phi_{sub} \rangle$$

# The antimatter sky - coherent halo description wrt $\gamma$ -rays



Compute fluxes and boosts à la Lavalley et al. 2008

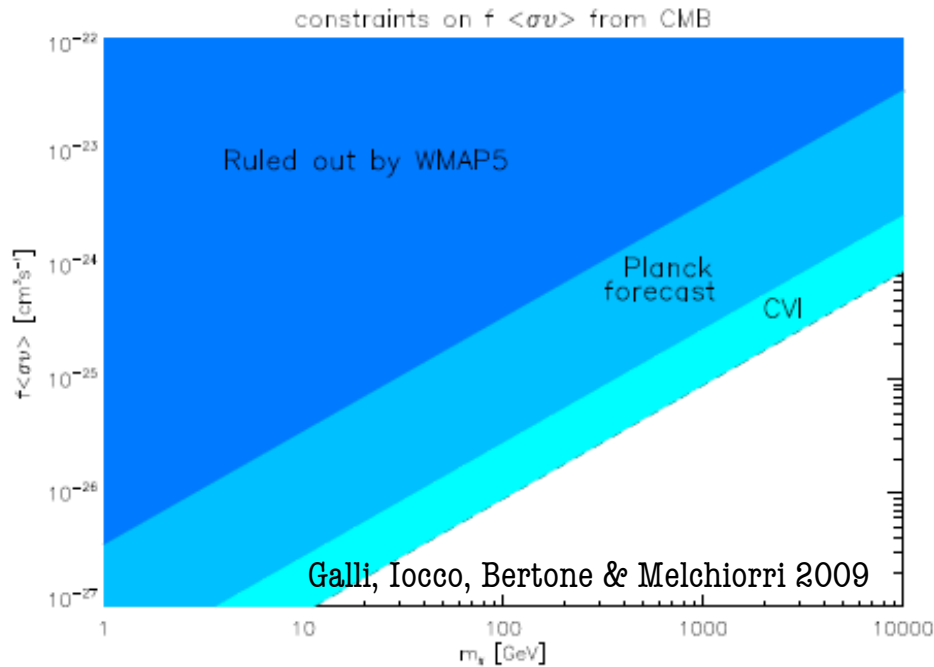
LP, Lavalley, Bertone & Branchini 2009

$$\phi_{CR,sm}(E_{CR}) \propto \langle \sigma v \rangle \int_{E_{CR}}^{\infty} dE \frac{dN_{CR}}{dE} \int_{diff.zone} d^3\bar{x} \left( \frac{\rho_{sm}(\bar{x})}{\rho_{sun}} \right)^2 G_{sun}^{CR}(\bar{x}, \lambda_D)$$

$$\langle \phi_{CR,cl} \rangle (E_{CR}) \propto \langle \sigma v \rangle N_{cl} \int_{E_{CR}}^{\infty} dE \frac{dN_{CR}}{dE} \int_{diff.zone} d^3\bar{x} \langle \xi \rangle_M(R) \frac{dP_V}{dV}(R) G_{sun}^{CR}(\bar{x}, \lambda_D) = N_{tot}^{sub} \langle \phi_{sub} \rangle$$

# Constraints from CMB - no structure dependence -

Injection of DM annihilation around  $z=1000$   
would affect recombination and hence modify the CMB

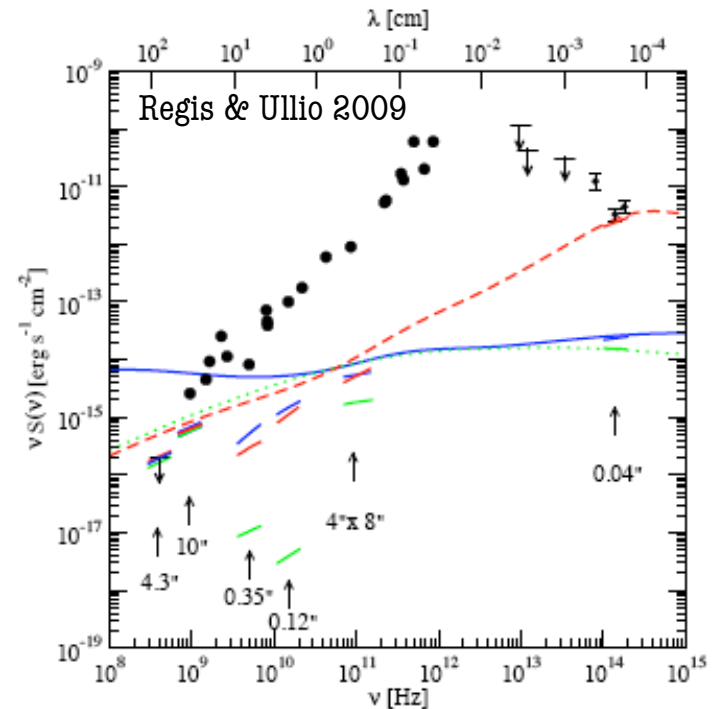


# The radio sky GC modeled coherently with $\gamma$ -rays and antimatter

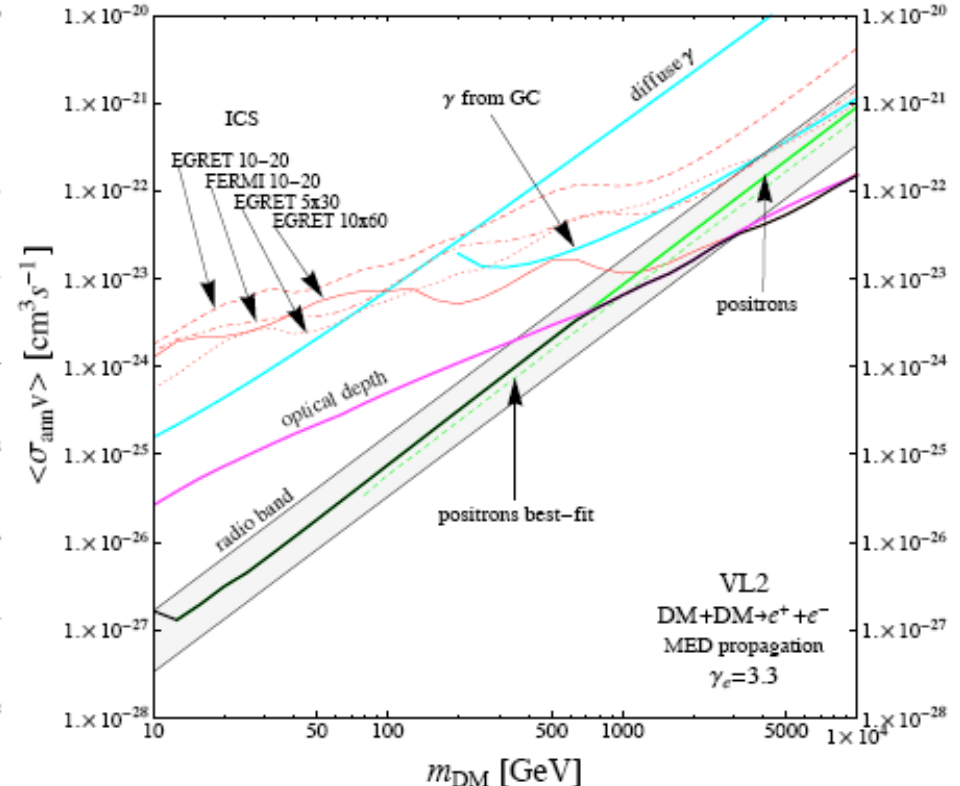
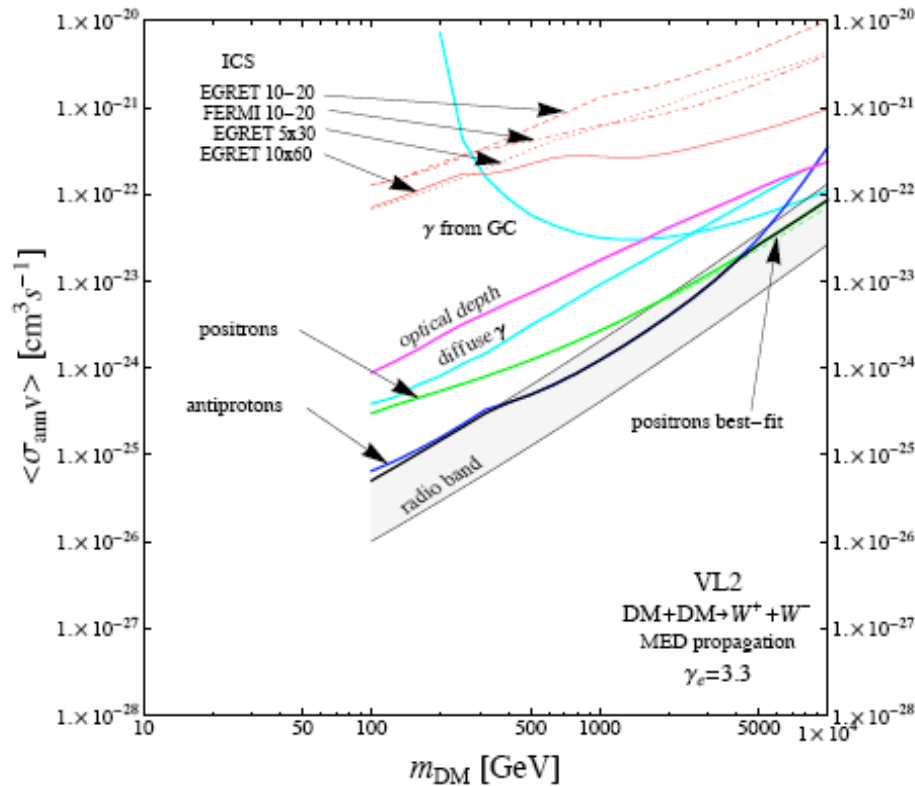
Compute synchrotron power

$$n_{e^\pm}(\bar{x}, E_{e^\pm}) = \frac{\sigma v}{2m_{\text{DM}}^2} \rho_{\text{DM}}^2(\bar{x}) \frac{N_{e^\pm}(> E_{e^\pm})}{b_{\text{syn}}(\bar{x}, E_{e^\pm})}$$

$$\nu \frac{dW_{\text{syn}}}{d\nu} = \frac{\sigma v}{2m_{\text{DM}}^2} \int_{\Delta\Omega} d\Omega \int_{\text{los}} ds \rho_{\text{DM}}^2(\bar{x}) E(\bar{x}, \nu) \frac{N_{e^\pm}(> E_{e^\pm})}{2}$$



# Multi<sup>3</sup> constraints on annihilation cross-section

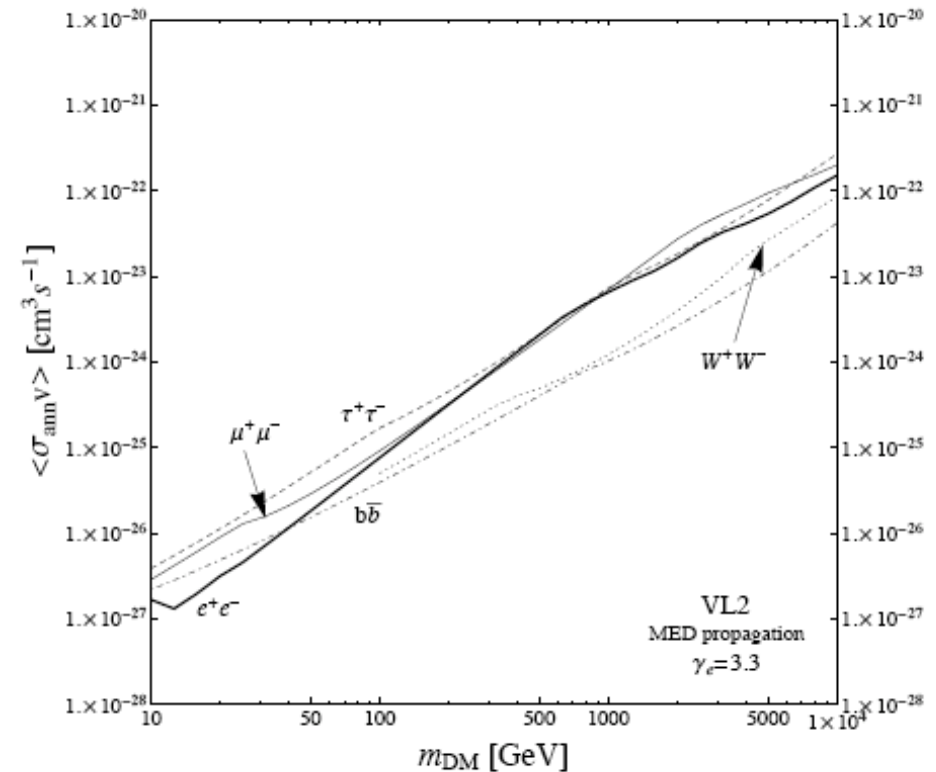
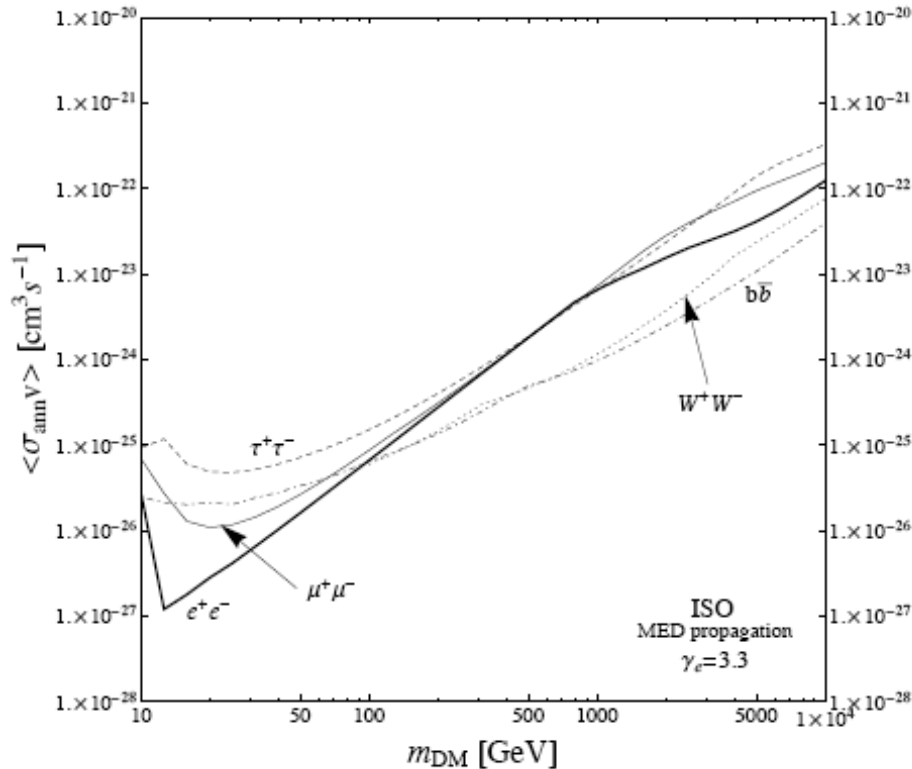


Catena, Fornengo, Pato, LP & Masiero 2010

Different messenger play different roles for different channels  
 Yet the amount of exclusion is almost the same..



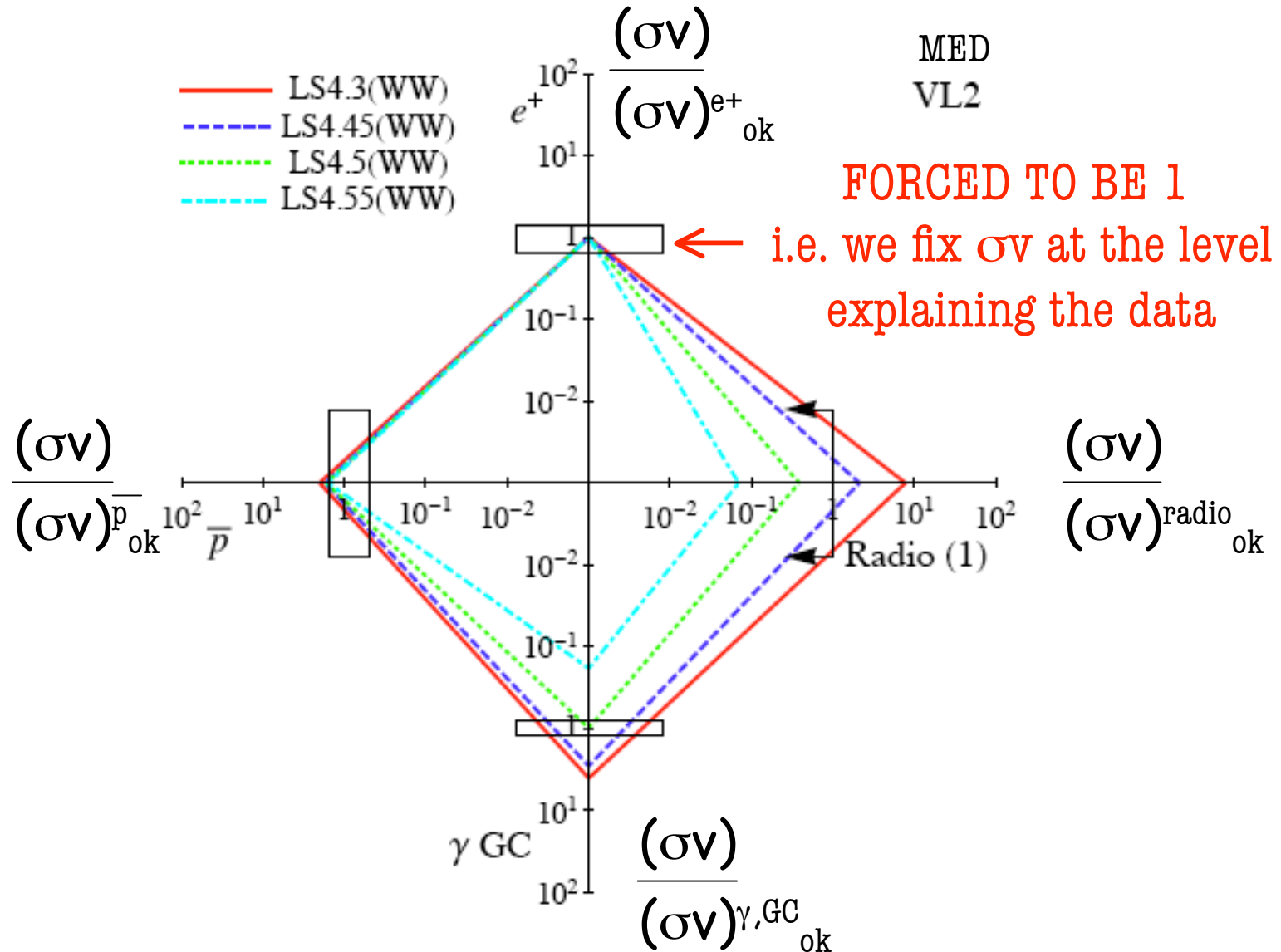
# Multi<sup>3</sup> constraints on annihilation cross-section



Catena, Fornengo, Pato, LP & Masiero 2010

In order to get bands of exclusion we change profile  
(Via Lactea II or Aquarius with subhalos, isocored without subhalos) and  
propagation parameters (inside the MIN-MED-MAX propagation model)

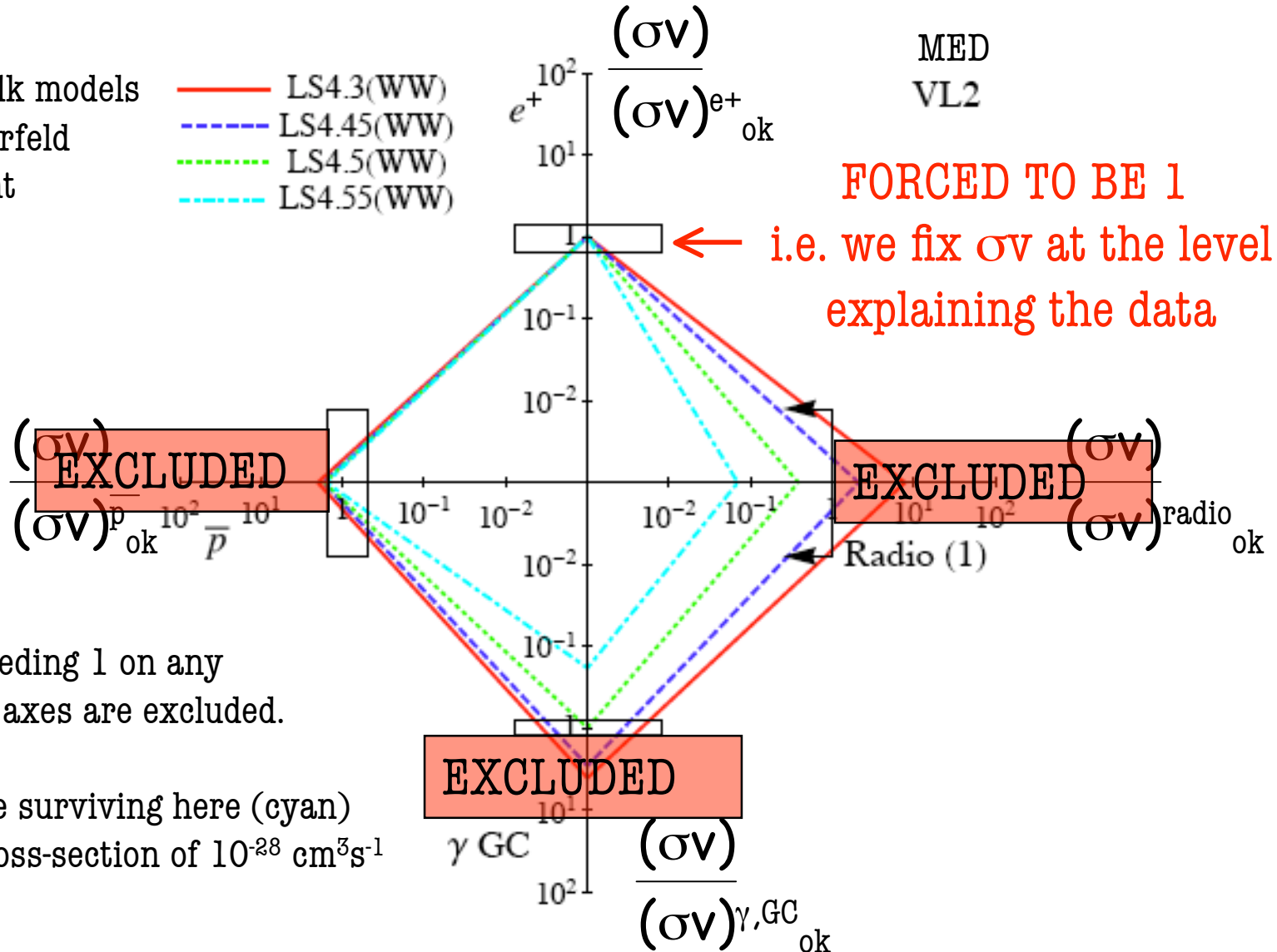
# Compact way of plotting multi-wavelength constraints APPLIED TO POSITRON FRACTION



# Compact way of plotting multi-wavelength constraints APPLIED TO POSITRON FRACTION

Lattanzi&Silk models  
with Sommerfeld  
enhancement

- LS4.3(WW)
- - - LS4.45(WW)
- ⋯ LS4.5(WW)
- · - · LS4.55(WW)

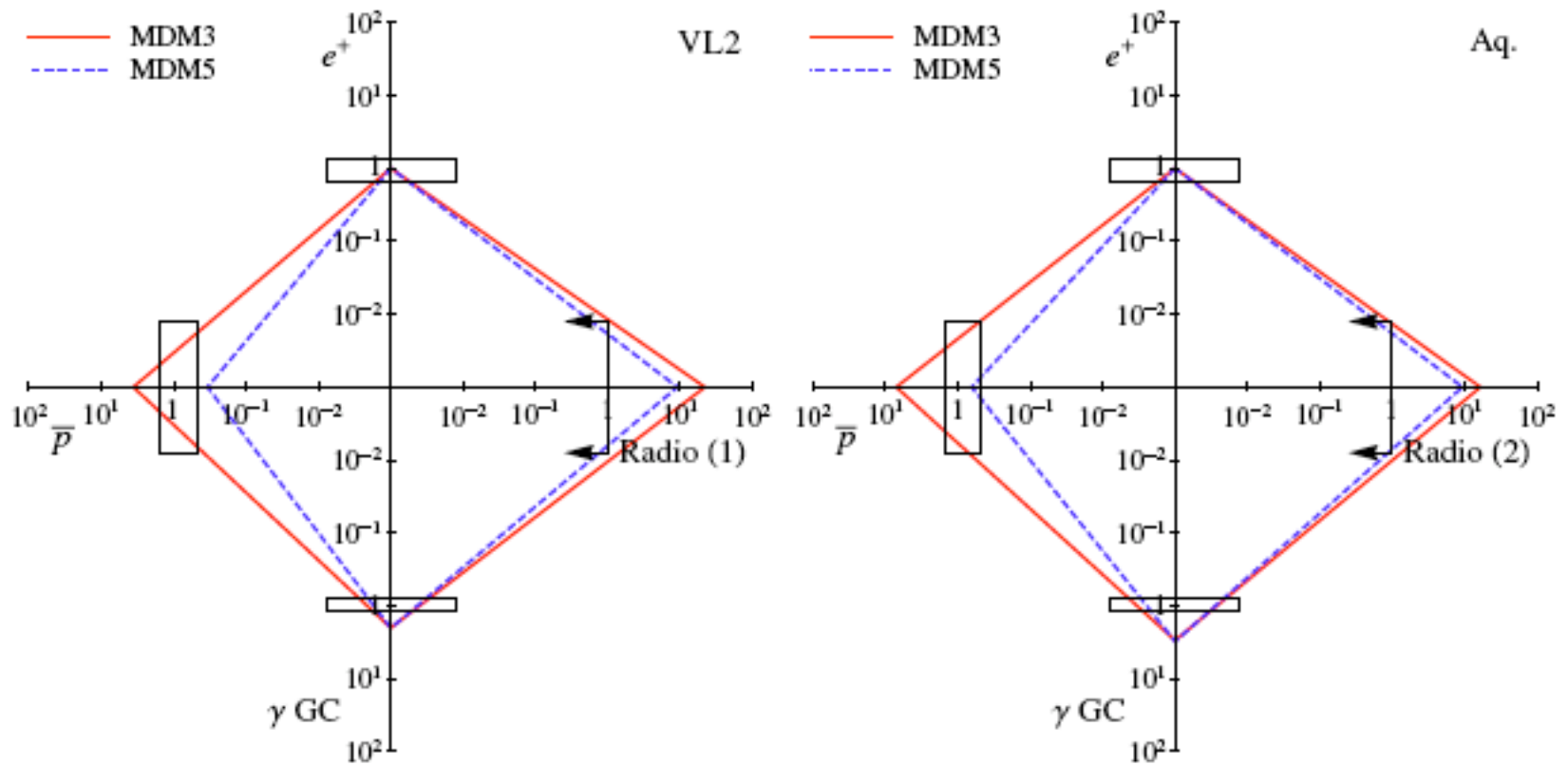


Models exceeding 1 on any of the other axes are excluded.

The only one surviving here (cyan) has got a cross-section of  $10^{-28} \text{ cm}^3 \text{ s}^{-1}$

# Compact way of plotting multi-wavelength constraints APPLIED TO POSITRON FRACTION

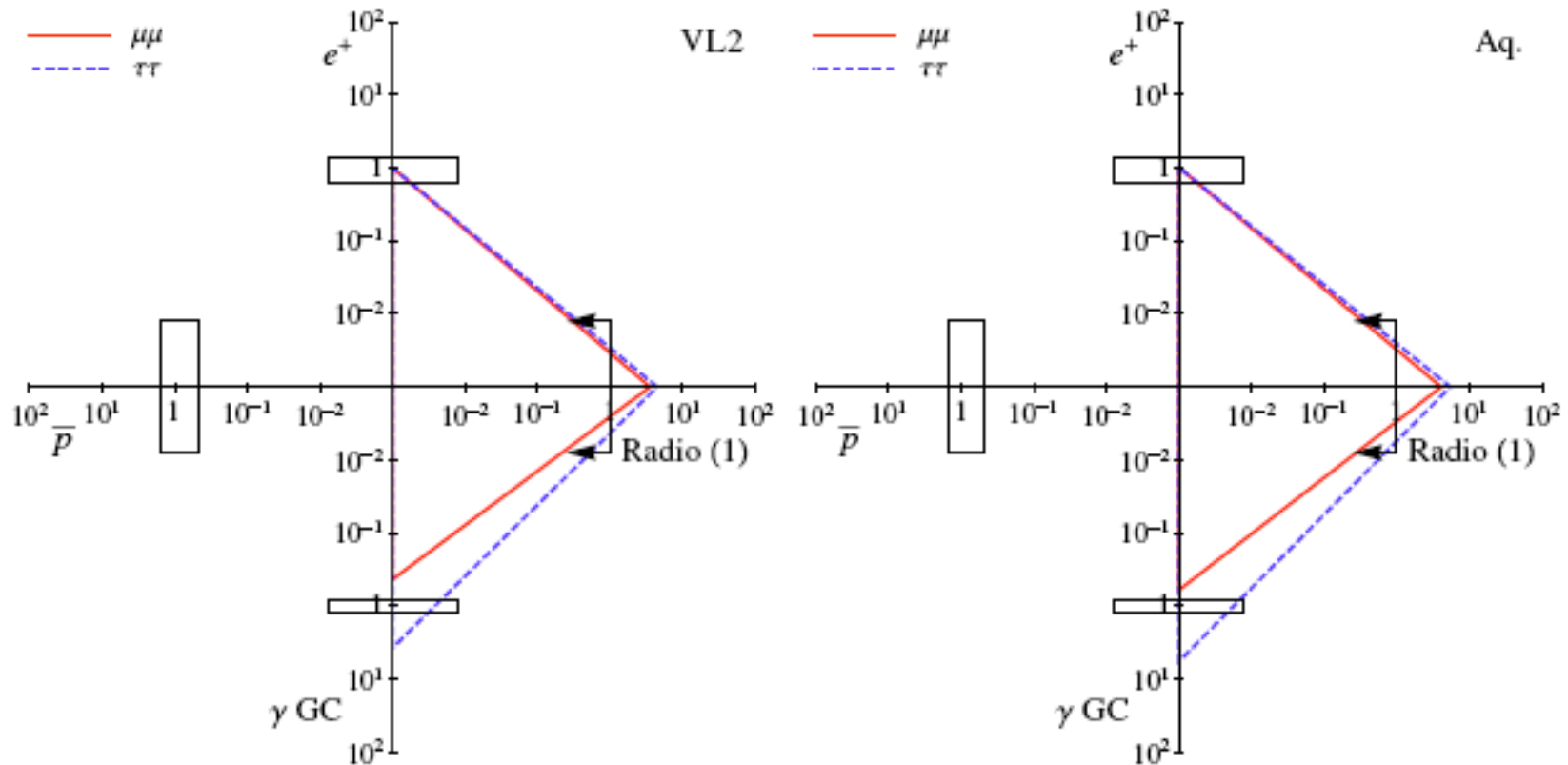
Minimal Dark Matter models are excluded





# Compact way of plotting multi-wavelength constraints APPLIED TO POSITRON FRACTION

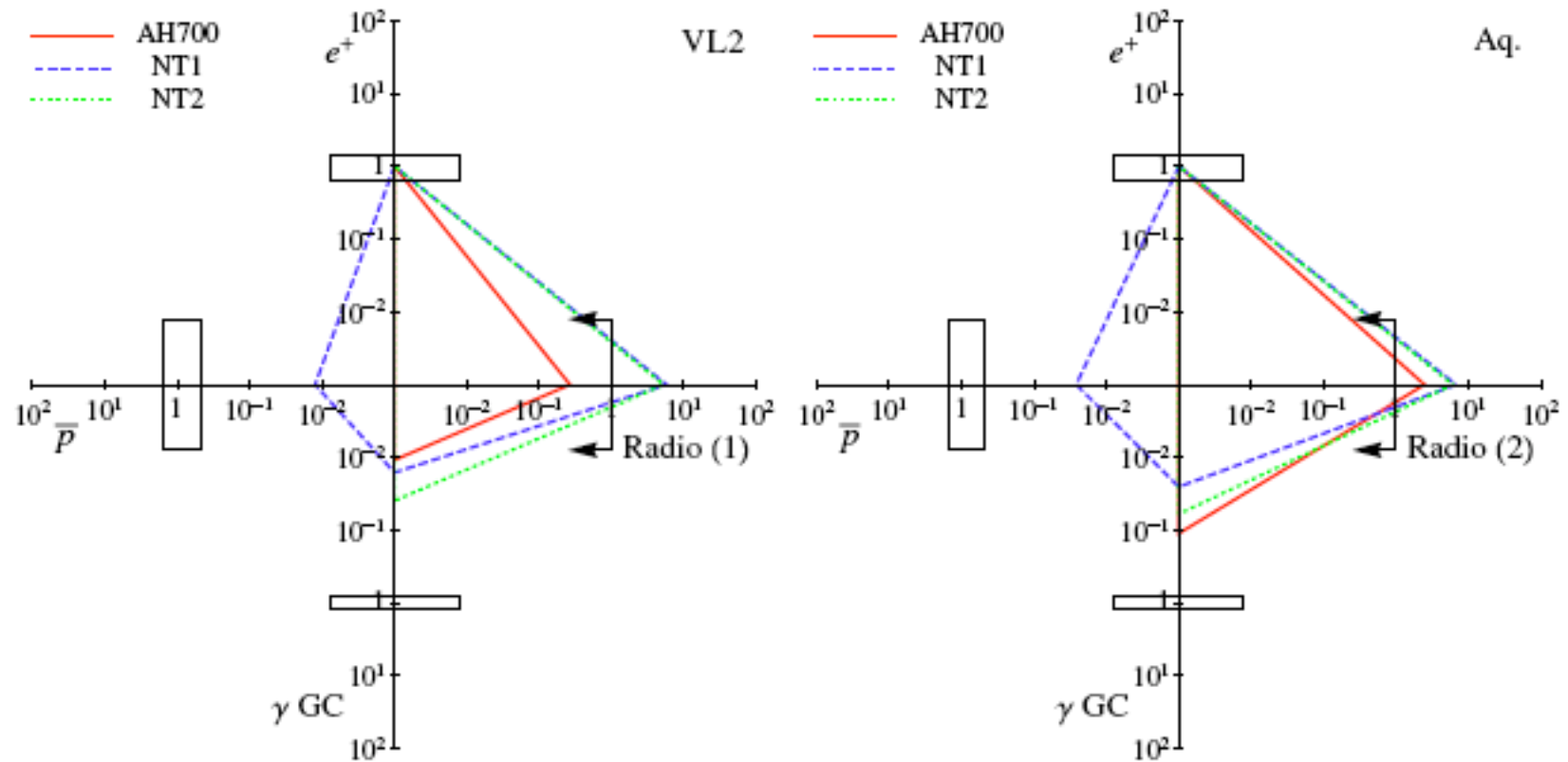
Leptonic models are excluded



# Compact way of plotting multi-wavelength constraints APPLIED TO POSITRON FRACTION

Nomura&Thaler models are excluded

Arkani-Hamed et al. model is the only one surviving



## **Conclusions**

**Multi<sup>3</sup> analysis must be applied to any candidate claimed to explain any excess**

**In the case of Coma, it proved that the DM explanation of the radio halo is possible only under favourable environment (profile and propagation)**